Geoacoustic Model of the Strait of Korea

K. B. Briggs
K. M. Fischer
Seafloor Geosciences Division
Ocean Science Directorate

Approved for public release; distribution is unlimited. Naval Oceanographic and Atmospheric Research Laboratory, Stennis Space Center, Mississippi 39529-5004.

These working papers were prepared for the timely dissemination of information; this document does not represent the official position of NOARL.

Abstract

Understanding the geology of the Strait of Korea is critical in making predictions of acoustic response because the region is a shallow-water, bottom-interacting area. The sediments are predominantly terrigenous with a significant marine biogenic component and exhibit a wide range of textures. In general, sediments are distributed along the axis of the strait by means of strong currents that winnow fines and leave predominantly coarser material as the lag deposit. However, a conspicuous mud belt of silty clay derived from nearby rivers persists near the Korean shore. This deposit thins toward the center of the strait where relict fine and medium sands are exposed. On the Japan side of the strait, hydrodynamic stress from currents waft away finer sediment to expose rock and leave coarse material such as shells in surface sediments. Over most of the strait, recent sea level changes have produced a middepth reflector beneath unconsolidated surface sediments. This acoustic horizon demarcates the surface of previously subaerially exposured marine sediments. Below the approximately 1 km thick layer of sediments in the strait, acoustic basement is rough due, in a large part, to the extensional tectonism associated with the back-arc-basin environment of the nearby Sea of Japan. Acoustic basement consists of folded sandstone or faulted basalt with extrusively and intrusively emplaced volcanic rock.

In this study, the sea floor of the strait is differentiated into 17 provinces based on sediment type, sediment thickness, and presence or absence of layering. A transect from the Goto Islands in Japan to the Kohung Peninsula in Korea was selected to model in detail. This transect traverses four of the largest geoacoustic provinces and samples the range of environments found within the strait. Acoustic property data as a function of depth in the sediment are supplied for each province for use as input parameters to acoustic field models that incorporate the variation of sediment physical properties with depth.

Acknowledgments

We thank Drs. Dawn Lavoie and Michael Richardson for supplying pertinent references and helping with the construction of the geoacoustic models. We are grateful to Dr. Allen Lowrie, NAVOCEANO, for sharing his knowledge of the geology of the area and for access to interpretive maps representing his synthesis of several published data sources. This study was supported by Program Element 0601153N, Dr. Robert Field, NOARL Code 244, Program Manager, Dr. E. R. Franchi, Block Manager.

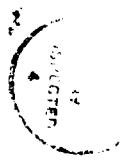

Contents

Introduction	1
Geology	1
Setting	1
Sediment Type	3
Sediment Thickness	4
Sediment Variability	7
Geoacoustic Provinces	8
Province 7	10
Province 17	12
Province 8	14
Province 9	17
Model Applicability	19
References	21
Figures	23
Appendix A: Model of Monet and Greene	40
Province Characteristics	41
Province Locations	42
Bottom/Water Velocity Ratios	43
Appendix References	44

GEOACOUSTIC MODEL OF THE STRAIT OF KOREA

INTRODUCTION

This technical note presents a general geological description of the Strait of Korea, including to a lesser extent the adjacent basins on either side of the strait, i.e., the Sea of Japan, the Yellow Sea and the East China Sea. Based on the regional geology, the strait was divided into provinces according to three sediment factors: textural classification, total thickness, and presence or absence of layering. Acoustic properties as a function of depth in the sediments are estimated for each province by utilizing literature data in combination with predictive modeling based on empirical relationships derived by Hamilton and other authors. The sediment properties deemed important are the following: compressional wave velocity, compressional wave attenuation, shear wave velocity, shear wave attenuation, and wet bulk density.

GEOLOGY

Setting

The Strait of Korea divides the peninsula of Korea from the Japanese islands of Honshu and Kyushu (Fig. 1). The strait, also referred to as the Tsushima Strait, is approximately 185 km wide, averages about 45 m deep, and includes several islands, among the largest of which are the islands comprising Tsushima. The widest point of the strait is 200 km and the greatest depth is 230 m in the Korean Trough located immediately west of Tsushima (Figs. 2 and 3). Tsushima divides the strait into the deeper western channel and the shallower, gently sloping eastern channel. The Strait of Korea is bordered to the southwest by the Yellow Sea, to the south by the East China Sea, and to the north by the Sea of Japan. Water depths drop off relatively gently toward the East China Sea but exhibit a steeper gradient toward the abyssal depths of the Sea of Japan (Fig. 2).

The Nakdong River, emptying just west of Pusan (Fig. 3) is the main source of sediments in the Strait of Korea, delivering about 5×10^6 kg of sediment annually (CHOUGH,

1983). Additional sediment input originates from the Yangzte River in China and is delivered into the strait by a northeasterly flowing arm of the Kuroshio Current called the Tsushima Current. Surface sediments in the strait are clayey silts close to the coast, but medium to coarse shelly sands cover the deepest parts of the strait (Fig. 4; CHOUGH *et al.*, 1991). This increase in grain size results from the winnowing of mud and very fine sand along the strait axis by the Tsushima Current, which attains a flow of up to 1.2 kt. The sea floor between Tsushima and Japan is largely sand with a few isolated patches of exposed rock (SHEPARD *et al.*, 1949). Tsushima is surrounded by a continuous belt of rock. Seismic records indicate a sediment thickness of 900 to 1000 m in the main channel of the strait. The total thickness of the sediment column thins with distance from the axis of the strait (Fig. 5). Biogenic calcium carbonate may constitute a significant (up to 60%, but averaging about 30%) portion of the sands.

Oceanographic conditions in the strait vary seasonally. The warm, saline, northeasterly flowing Tsushima Current is strongest during the summer months. This current weakens during the winter months due to strong, northwesterly winds. The northwesterly winds enhance the West Korean Coastal Current, which delivers cooler, less saline waters from the Yellow Sea into the strait. Consequently, a coastal front develops during winter at the boundary between the two water masses delivered by these currents (PARK, 1983). Surface salinity averages 35.0 ppt in spring, dropping to 32.5 ppt in late summer (NAVAL OCEANOGRAPHIC OFFICE, 1974). Bottom water salinity remains relatively homogeneous throughout the year below 60 m with values ranging from 34.0 ppt to 34.1 ppt. Bottom water temperature averages 15°C in the winter when the water column is well mixed. In the summer, a strong thermocline develops, with bottom water temperatures ranging from 16.5 to 10°C depending on the depth of the seafloor in the strait (JAPAN OCEANOGRAPHIC DATA CENTER, 1968; 1971). Figure 6 depicts typical sound velocity data for the Sea of Japan near the Strait of Korea. Using an average midchannel water depth of 125 m, bottom water velocity averages 1482 m/s and ranges between 1458 and 1509 m/s.

Sediment Type

As a result of the hydrodynamic action of waves and currents, the sediments of the Strait of Korea are significantly coarser than the sediments found in the seas flanking the strait. (The exception to this generalization is the fine-grained mud found near shore on the Korean side of the strait.) The shelf sediments of the East China and Yellow Seas are mainly silts, ranging from very fine to medium silts (KELLER and YE, 1985). The surface silts and clays of the East China and Yellow Seas are modern sediments deposited over relict shelf sand of Pleistocene age (BUTENKO *et al.*, 1985). Surface sediments in the Yellow Sea as far south as Cheju Island (Cheju Do; Fig. 1) are sands with porosities near 50% and wet bulk densities of 1.7 g/cm^3 (KELLER and YE, 1985). Sediments of the Sea of Japan proximal to the strait are fine silts to clays. Laminae, graded bedding, and occasional gravel are found in cores from the Tsushima Basin, located to the north of Tsushima, indicating slumping of shallower shelf and strait sediments and resultant deposition via turbidity currents (NAVAL OCEANOGRAPHIC OFFICE, 1974; CHOUGH *et al.*, 1985). The high organic matter content (5-10%) and the high water content of these fine-grained, terrigenous sediments are responsible for the low bulk density of sediments found on the slope leading to the Sea of Japan and within Tsushima Basin (LEE *et al.*, 1991).

Surface sediment in the strait shows a zonal distribution (Fig. 4). Mud (silty clay or clayey silt) prevails along the coastal embayments and rias of the Korean peninsula extending to water depths of 60 m. Grain size analysis available for the nearshore muds show a mean size of 7 to 8ϕ (0.008 to 0.004 mm). Sediment porosity varies between 56 to 72% and calcium carbonate makes up 3 to 15% of the material by weight. An increasing proportion of clay in sediments at water depths of 30 to 100 m decreases the mean grain size from 7 to 9ϕ and increases the porosity from 67 to 80%. Organic matter content in these nearshore muds is high (8 to 12%) and contributes to low wet bulk density. Between the zone of nearshore muds near Korea and the islands of Tsushima, a belt of coarser sediments ranging from sandy muds through gravelly sand line the bottom of the strait (CHOUGH *et al.*, 1991). Porosities vary between 35 and 44% and calcium carbonate fractions make up 10 to 40% of the sediment by weight. Layers of

muddy sand representing horizons associated with eustatic sea level changes are found at various depths in the sediment, the shallowest at 1 mbsf (CHOUGH *et al.*, 1991).

A zone of mud (sandy silt to sandy silty clay) is also found to the northeast of Tsushima. This muddy region may represent a kinetic energy "shadow" to the northeast of Tsushima, i.e., drag caused by the diversion of current flow around these islands results in a loss of competence with the resulting settling of finer material in this area. Beyond Tsushima, the eastern channel consists of shelly sand, indicating an increase in the competence of flow. In the easternmost part of the strait, a thin veneer of fine sand overlying rock surrounds the Goto Archipelago (Goto Retto; Fig. 1), Iki Island, and Kyushu Island.

Concentration of calcium carbonate and organic matter in the sediments of the strait have only a small influence on bulk density; textural characteristics of the sediment control the porosity and thereby the bulk density. Well-rounded gravels found on the midshelf and in the Korean Trough are volcanic in origin and may constitute up to 20% of the sediment, thereby increasing the average grain density (PARK and YOO, 1988). Clay minerals present in the strait are predominantly illite (PARK and KHIM, 1990).

Sediment Thickness

Three factors strongly influence sediment thickness in the Strait of Korea: bottom topography, rate of sediment supply, and currents. The approximately kilometer-thick layer of sediments in the strait overlies rough basement rock of complex tectonic history (Fig 7). The basement under the western channel of the strait is probably part of the Fukien-Reinan massif and consists of both olivine basalt and sandstone (MONET and GREENE, 1985). The eastern channel basement consists of folded sedimentary and acidic intrusive rocks of Tertiary age (Fig. 8a; Table 1). The rough basement is an extension of the regional offshore topography of submerged hills to the south and faults, ridges and troughs parallel to the shore of Japan to the north (LUDWIG *et al.*, 1975). The eastern side of the strait is strongly influenced by the tectonics of the Sea of Japan, which is a back-arc-basin environment. This environment is characterized by intrusive and extrusive volcanic rocks, of which large-scale bottom roughness, numerous acoustic reflectors and

Table 1. Stratigraphy for region shown in Fig. 8a. (Table from Katsura and Nagano, 1976. Translation of Japanese by K. M. Fischer.)

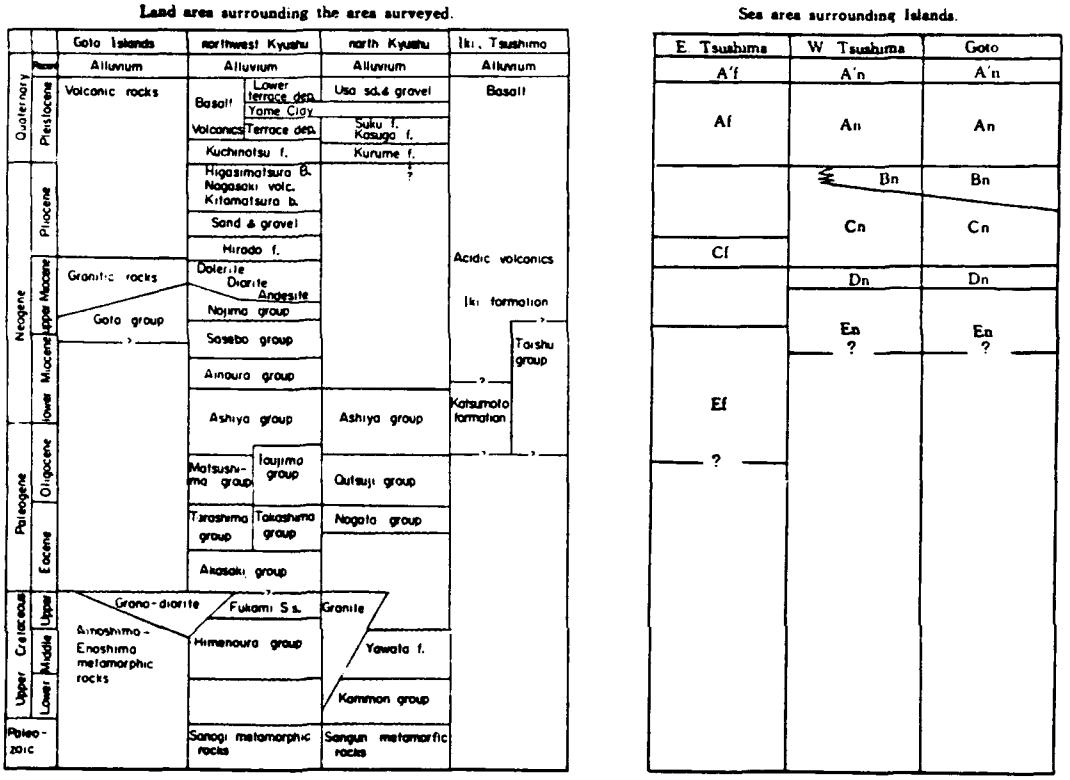

Translation:

A 層	上部第四系	Recent
B 層	下部第四系	Pleistocene
C 層	鮮新統	Pliocene
D 層	上部中新統	upper Miocene
En 層	中～下部中新統（五島層群相当層）	mid to lower Miocene (corresponding to Goto group)
Ef 層	下部中新統以下（対州層群相当層）	lower Miocene to Oligocene (corresponding to Taishu group)

islands are manifestations (Fig. 8). The western side of the strait has a significantly higher supply of sediment from drainage of a larger continental area by rivers than the Japan side of the strait. The middle of the strait is shallow, and, therefore, sedimentation in this area is strongly influenced by the fast-flowing Tsushima Current.

The strait sediments are relatively thin compared to the immense accumulation of river-derived sediments in the Yellow and East China Seas flanking the strait to the south and compared to the turbidites and pelagic sediments of the Tsushima Basin in the Sea of Japan flanking the strait to the north. LUDWIG *et al.* (1975) describes the strait as a region of ridges and troughs blanketed with sediments. Seismic profiles of the region of the strait opening into the Sea of Japan show strong surface reflectors with little or no penetration into the bottom, probably indicating the coarse nature of sediments in the strait (NAVAL OCEANOGRAPHIC OFFICE, 1974).

Sediment thickness as determined by seismic reflection profiles (Fig. 9) varies from 320 m south of Tsushima Island to 1080 m in the middle of the strait lying between the southernmost tip of Honshu and the Korean peninsula (LUDWIG *et al.*, 1975). The sediment thickens to 1870 m as one progresses into the Tsushima Basin (1500 m water depth). Most of the sediments are unconsolidated sands with interval velocities of 1650-1970 m/s, but in some cases the sea floor presumably is exposed mudstone with interval velocities of 2200-2822 m/s. Profiles in the northern part of the strait and near the peninsula show unconsolidated sediment thicknesses of 510-1260 m with interval velocities of 1750-1940 m/s.

Nearshore muds (Fig. 10) derived from the outflows of the Nakdong River and the Somijn River comprise a layer 30 to 50 m thick that thins offshore toward a region of exposed relict sands (PARK and YOO, 1988). Total sediment accumulation nearshore can reach 50 m including underlying relict sands. The mid- and outer shelves are covered by coarse-grained material with some gravels and shell fragments from the postglacial transgression and are as thin as 5 m thick near the Korea Trough. A major reflector is present throughout the sedimentary sequences in the inner shelf (Fig. 11). This horizon of high acoustic impedance represents an erosional discontinuity that occurs at a progressively shallower depth offshore and ultimately reaches the sediment surface on

the midshelf. The origin of this reflector is thought to be the result of subaerial exposure of the strait sediments during the most recent (late Pleistocene) sea level regression (Fig. 12). There are acoustically turbid areas within this lower sedimentary sequence and is thought to represent entrapped gas (Fig. 11b; PARK and YOO, 1988).

Large-scale sand ridges and asymmetrical sand waves occur on the midshelf between 70 and 80 m water depth, with a height of 12 m and wavelengths of about 2.5 km. Sharp-crested sand waves are found at water depths between 100 and 120 m. These bedforms have a height of less than 3 m and wavelengths about 0.1 to 0.3 km (PARK and YOO, 1988).

Sediment Variability

Lateral variability of sediment texture is a function of the hydrodynamic characteristics of the strait. The strong, northeastward flow of the Tsushima Current through the strait creates and maintains textural differences that distinguish elongate zones of sediment type lying parallel to the southwest-northeast axis of the strait (Fig. 4). The winnowing action of the current removes much of the fine-grained sediment and deposits the fines in areas where the current loses competence, such as the slope and basin of the Sea of Japan and the region to the northeast of the islands of Tsushima. In areas where the current reaches the bottom at least seasonally, only the coarsest sediments remain. Since physical properties vary with grain size, compressional wave velocity and attenuation change as well, and these changes ultimately affect acoustic response. Due to the nature of the variability described above, spatial variability of acoustic properties will be especially apparent *across* the strait as opposed to down its axis.

Sediment thickness varies to the greatest extent across the strait as well. Huge accumulations of terrigenous material exist near the outflows of rivers on the Korean peninsula due to the protection from the strongest currents afforded by the ria-type topography of the drowned valleys and submerged hills along this coast. The thickness of unconsolidated sediments is quite variable on the eastern side of the strait due to the proximity of acoustic basement to the sediment surface (Fig. 8). Near the Goto Islands,

thin veneers of coarse and medium sand overlie shallow reflectors that are probably intrusive basalt and folded sandstones. The roughness of the basement underlying the sediments also affects the sediment thickness; sediment fills the areas of depressed topography, e.g., faults and troughs, while leaving the elevated ridges thinly veneered with sediment. Additionally, rough basement contributes variability by providing many obliquely oriented surfaces for acoustic scattering.

GEOACOUSTIC PROVINCES

The variability of sediment distribution as outlined above makes the Strait of Korea a complex region to model. By simplifying the model of Monet and Greene (1985; Appendix I), the strait can be divided into 17 geological provinces (Fig. 13) based on sediment texture, total thickness and presence or absence of layering (Table 2). Since it is beyond the scope of this investigation to generate an accompanying model for all 17 provinces, geoacoustic models were developed for 4 of the most areally extensive and most diverse provinces in the strait. These provinces lie along a hypothetical transect from the Goto Islands of Japan on the eastern side of the strait to the Kohung peninsula of Korea on the western side of the strait (Fig. 13). The provinces are discussed in the order in which they are encountered as one progresses from the eastern side to the western side of the strait.

Values for geoacoustic parameters for each major stratum of each province are given in accompanying tables. The parameters of interest and the notation used for each are described below:

compressional wave velocity at the sediment surface, $V_{p\underline{0}}$, in m/s

compressional wave velocity with depth in the sediments, V_p, in m/s

shear wave velocity at the sediment surface, $V_{s\underline{0}}$, in m/s

shear wave velocity with depth in the sediments, V_s, in m/s

compressional wave attenuation at the sediment surface, $K_{p\underline{0}}$, in dB/m/kHz

compressional wave attenuation with depth in the sediments, K_p, in dB/m/kHz

shear wave attenuation at the sediment surface, K_{s0}, in dB/m/kHz

shear wave attenuation with depth in the sediments, K_s, in dB/m/kHz

sediment density, ρ, in g/cm^3

depth in the sediment, Z, in meters except where noted

Table 2. Geological provinces in the Strait of Korea depicted in Fig. 13. (Revised from MONET and GREENE, 1985.)

Province	Grain Size	Sediment Thickness	Layering
1	sandy silt	thick	Y
2	coarse sand	thick	N
3	silty clay	thick	N
4	silty sand	thick	N
5	fine sand	thick	N
6	sand-silt-clay	thick	Y
7	c. sand/rock	little/none	N
8	sand-silt-clay	thin	Y
9	silty clay	thin	Y
10	silty sand	thin	N
11	gravelly sand	thin	N
12	sand-silt-clay	thick	N
13	clayey silt	thin	N
14	silty clay	thick	Y
15	fine sand	thin	Y
16	gravel/rock	little/none	N
17	shelly fine/med. sand	thick	Y

Province 7

Province 7 surrounding the Goto Islands (Fig. 13) is characterized by a thin cover of unlayered, coarse sediments with patches of exposed rock. The surface sediment layer of coarse, terrigenous sand is approximately 100 m thick nearshore and thins with increasing distance from land to expose basement rock. Uneven basement and thin sediment cover combine to produce a rugged seafloor in this province. Interpretation of surface sediments and underlying facies are made from Fig. 8 and Table 1.

The model for Province 7 (Table 3) is calculated by assuming a thin veneer of sand overlying basement, which is typical of the seafloor in this province. The following summarizes the derivation of values for acoustic parameters found in Table 2:

1. An average value of 1482 m/s for sound velocity of bottom water in the strait is used (Fig. 6).

2. The ratio of sediment velocity to bottom-water velocity is calculated as 1.201 from items 1 and 4.

3. The velocity ratio relative to bottom water for exposed rock is 3.43 (MONET and GREENE, 1985).

4. The compressional wave velocity at the sediment surface is assumed to be 1780 m/s, a value for coarse sands from HAMILTON and BACHMAN (1982).

5. The compressional wave velocity with depth in the sediments is calculated from the relation $V_p = KZ^{0.015}$, where K is 1862 m/s (HAMILTON, 1980).

6. Shear wave velocity is calculated using the empirical relationship between effective stress, void ratio and shear modulus developed by BRYAN and STOLL (1988) and subsequent calculation of velocity by RICHARDSON *et al.* (1991). Laboratory values are converted to field velocities (lab × $\sqrt{2}$) as suggested by STOLL *et al.* (1987). Void ratio is calculated from the density in the table and an assumed value of 2.65 g/cm^3 for grain density.

7. The compressional wave attenuation at the sediment surface is estimated to be 0.53 dB/m/kHz from values for coarse sand given by HAMILTON (1972).

8. The compressional wave attenuation with depth in the sediments is calculated from the relation $K_p(Z) = [(K_{p0} - 0.214)/0.236]\ [0.45Z^{-1/6} - 0.214 + 0.00014Z] + 0.214$

— 0.00014Z (HAMILTON, 1980).

Table 3. Geoacoustic Model for the Strait of Korea, Province 7.

	Depth (m)	V_p (m/s)	V_s (m/s)	K_p (dB/m/kHz)	K_s (dB/m/kHz)	ρ (g/cm^3)
Bottom Water	30-120	1482				
coarse	surface	1780	133	0.53	18.9	2.03
sand	5	1907	250	0.39	13.9	2.03
	10	1927	292	0.34	12.1	2.03
	15	1939	320	0.31	11.1	2.03
	20	1947	341	0.29	10.3	2.03
	25	1954	359	0.28	10.0	2.03
	50	1974	419	0.24	8.6	2.03
	75	1986	459	0.22	7.8	2.03
	100	1995	490	0.21	7.5	2.03
Acoustic Basement (Tertiary Basalt)		4080	2001	0.02	0.07	2.35

9. The shear wave attenuation at the sediment surface is assumed to be 18.9 dB/m/kHz (HAMILTON, 1980).

10. Shear wave attenuation with depth in the sediment is calculated from the empirical relation, $K_s(Z) = K_p(Z)(K_{s0}/K_{p0})$, where Z is depth in units of choice (HAMILTON, 1980).

11. Density of coarse sand as given by HAMILTON (1980) is 2.03 g/cm^3. No change in density due to consolidation with increasing overburden pressures is assumed.

12. Values for acoustic basement are calculated from HAMILTON (1980) based on

seismic refraction data from LUDWIG *et al.* (1975).

Province 17

Province 17 is the largest province in the strait and can be used to characterize the seafloor of the channel lying to the east of Tsushima (Fig. 13). Surface sediments are fine to medium shelly sands ranging in thickness from as little as 5 m in the eastern portion of this province to as much as 180 m in the western portion; an average value of 90 m is used in the model. This surface layer has 2 to 4 reflection horizons embedded in what appears to be otherwise uniform material. In the westernmost region of this province, the surface sediments cover a semiconsolidated silty sand that is probably Pleistocene in origin (Fig. 12). The semiconsolidated sediment may extend to acoustic basement; seismic refraction profiles by LUDWIG *et al.* (1975) indicate a 320 m layer of relatively low velocity sediment lying over acoustic basement. The interval velocity of the basement is estimated at 4130 m/s and probably consists of intruded Tertiary basalt and sedimentary rock.

The geoacoustic model for Province 17 presented in Table 4 was constructed as follows:

1. An average value of 1482 m/s for sound velocity of bottom water in the strait is used (Fig. 6).

2. An average velocity ratio of 1.20 is determined from surface sediment maps provided by the NAVAL OCEANOGRAPHIC OFFICE (A. LOWRIE, personal communication) and MONET and GREENE (1985).

3. The compressional wave velocity at the sediment surface is calculated as 1778 m/s from items 1 and 2 above.

4. The compressional wave velocity with depth in the sediment is calculated from $V_p = KZ^{0.015}$, where K is 1860 m/s (HAMILTON, 1980).

5. Shear wave velocity with depth in the sediment is calculated using the empirical relationship between effective stress, void ratio and shear modulus developed by BRYAN and STOLL (1988) and the subsequent calculation of velocity by RICHARDSON *et al.* (1991). Laboratory values are converted to field velocities (lab × $\sqrt{2}$) as suggested by STOLL *et*

al. (1987). Void ratio is calculated from the density in the table and an assumed value of 2.65 g/cm^3 for grain density.

6. Compressional wave attenuation in the surface sediment is estimated to be 0.45 dB/m/kHz using an average value for fine and medium sands (HAMILTON, 1972).

Table 4. Geoacoustic Model for the Strait of Korea, Province 17.

	Depth (m)	V_p (m/s)	V_s (m/s)	K_p (dB/m/kHz)	K_s (dB/m/kHz)	ρ (g/cm^3)
Bottom Water	20-50	1482				
shelly	surface	1778	121	0.45	13.2	1.96
fine	5	1906	229	0.34	10.0	1.96
to	10	1926	267	0.31	9.1	1.96
medium	15	1937	296	0.29	8.5	1.97
sand	20	1946	316	0.27	7.9	1.97
	25	1952	336	0.26	7.6	1.98
	50	1973	398	0.23	6.7	1.99
	75	1985	441	0.22	6.5	2.00
semi-	100	1993	486	0.21	6.2	2.03
consolidated	125	2000	521	0.20	5.9	2.05
silty	150	2005	553	0.20	5.7	2.07
sand	200	2014	598	0.19	5.6	2.08
	250	2021	635	0.18	5.3	2.09
	300	2026	669	0.17	5.0	2.10
Acoustic Basement (Tertiary Basalt)		4130	2027	0.02	0.07	2.35

7. Compressional wave attenuation with depth in the sediment is calculated using the relation $K_p(Z) = [(K_{p0} - 0.214)/0.236]\ [0.45Z^{-1/6} - 0.214 + 0.00014Z] + 0.214 - 0.00014Z$ (HAMILTON, 1980).

8. Shear wave attenuation in the surface sediment is assumed to be 13.2 dB/m/kHz.

9. Shear wave attenuation with depth in the sediment is proportional to compressional wave attenuation according to the empirical relation $K_s(Z) = K_p(Z)(K_{s0}/K_{p0})$, where Z is depth in units of choice (HAMILTON, 1980).

10. The density of surface sediment assumed to be 1.96 g/cm^3. This value is typical of fine and medium shelly sands found on continental shelves (HAMILTON, 1980). The sediment densities at selected depths are based on representative values given by HAMILTON (1980).

11. Values for acoustic basement are calculated from HAMILTON (1980) based on seismic refraction data from LUDWIG *et al.* (1975).

Province 8

Province 8 is found at water depths between approximately 70 and 120 m off the Korean peninsula (Fig.13). This province, which occupies most of the western channel of the strait, represents a transitional region between deposits of nearshore modern silty clays and offshore relict sands (CHOUGH *et al.*, 1991). In this province, four sediment layers overlie acoustic basement. These layers are designated in Table 5 as: sand-silt-clay, medium sand, semiconsolidated silty sand, and unknown. The surface layer of Holocene sand-silt-clay is only 5 to 20 m thick near shore and thins with increasing distance from the shore; an average thickness of 10 m is used in Table 5. This surface layer is underlain by a deposit of medium-grained, relict sand approximately 10 m thick (PARK and YOO, 1988). A deeper reflector at 10 to 40 mbsf demarcates the surface of a third sediment layer that extends to 940 mbsf. Little is known about the lithology of this formation, but it may be a continuation of the semiconsolidated silty sand formation found at depth in the western section of Province 17. The upper surface of this formation is occasionally obscured by acoustically turbid zones that are thought to be methane gas.

Underlying this formation, a fourth sediment layer of unidentified lithology can be identified by an interval velocity of 2680 m/s from sonobu data. Acoustic basement is reached at 1620 mbsf with material having an interval velocity of 4650 m/s (LUDWIG *et al.*, 1975) and consists of sandstone and basalt.

Table 5. Geoacoustic Model for the Strait of Korea, Province 8.

	Depth (m)	V_p (m/s)	V_s (m/s)	K_p (dB/m/kHz)	K_s (dB/m/kHz)	ρ (g/cm^3)
Bottom Water	50-100	1482				
sand-	surface	1535	52	0.60	13.3	1.58
silt-	5	1542	97	0.43	9.5	1.58
clay	10	1548	114	0.37	8.2	1.58
medium	15	1804	286	0.43	10.0	2.00
sand	20	1813	312	0.42	9.3	2.00
	25	1910	364	0.42	9.3	2.10
semi-	50	1936	443	0.39	8.6	2.11
consolidated	100	1959	534	0.34	7.5	2.13
silty	200	1981	629	0.27	6.0	2.13
sand	500	2009	777	0.14	3.1	2.13
	1000	2600	1066	0.07	1.6	2.17
?	1500	2800	1222	0.04	0.9	2.20
Acoustic Basement (Sandstone-Basalt)		4350	2142	0.02	0.07	2.43

The geoacoustic parameters for Province 8 given in Table 5 are based on the following:

1. The sound velocity of bottom water is approximated as 1482 m/s from Fig. 6.
2. The velocity ratio of sediment relative to bottom water is estimated to be 1.036.

This value represents a compromise between typical values for sandy silty clays (to represent the uppermost layer) and typical values adjusted for consolidation due to overburden pressure for medium-grained sands (to represent the medium sand layer) (HAMILTON and BACHMAN, 1982).

3. The compressional wave velocity in the surface sediments is estimated to be 1535 m/s. This estimate is based on values for sandy silty clays given in HAMILTON and BACHMAN (1982).

4. Compressional wave velocity with depth is calculated for the four layers using empirically derived equations (HAMILTON, 1980): for the surface layer, $V_p = (1000)(0.001V_{p0} + 1.304Z - 0.741Z^2 + 0.257Z^3)$, where Z is depth in *kilometers*; for the medium sand layer, $V_p = KZ^{0.015}$, where K is 1736 m/s; for the layer of semiconsolidated silty sand and the deepest stratum, $V_p = KZ^{0.015}$, where K is 1830 m/s. Consolidation due to overburden pressure is taken into account where necessary.

5. Shear wave velocity with depth is calculated for the first three sediment layers using the empirically derived relationship between effective stress, void ratio and shear modulus of BRYAN and STOLL (1988) and subsequent calculation of velocity by RICHARDSON *et al.* (1991) Laboratory values are converted to field velocities (lab × $\sqrt{2}$) as suggested by STOLL *et al.* (1987). Void ratio is calculated from the density in the table and an assumed value of 2.65 g/cm^3 for grain density.

6. $V_s = 0.78V_p - 0.962$ for the deeper stratum of unidentified lithology.

7. Compressional wave attenuation in the surface sediment is estimated to be 0.60 dB/m/kHz using a value typical of sandy silty clay taken from HAMILTON (1972). For sediments lying between 15 and 450 m, K_{p0} is estimated to be 0.45 dB/m/kHz.

8. The compressional wave attenuation with depth is calculated as follows for the various layers using empirically derived relations for similar sediments (HAMILTON, 1980): $K_p(Z) = [(K_{p0} - 0.214)/0.236]\ [0.45Z^{-1/6} - 0.214 + 0.00014Z] + 0.214 - 0.00014Z$ for depths within the sand-silt-clay layer; $K_p(Z) = 0.214 - 0.00014Z - (0.214 - K_{p0})e^{-Z/200}$ for depths within the medium sand and semiconsolidated silty sand layers to 450 m; $K_p(Z) = 0.21 - 0.00014Z$ for depths from 450 to 790 m. The appropriate K_{p0} (see item 10) must be used.

9. Shear wave attenuation in the surface sediment is estimated to be 13.3 dB/m/kHz.

10. Shear wave attenuation with depth is calculated using the relation $K_s(Z) = K_p(Z)(K_{s0}/K_{p0})$, where Z is depth in units of choice (HAMILTON, 1980).

11. Sediment densities are estimated using representative values taken from HAMILTON (1978) and HAMILTON and BACHMAN (1982). Consolidation due to overburden pressure is taken into account for the two deeper layers.

12. Values for acoustic basement are calculated from HAMILTON (1980) based on seismic refraction data from LUDWIG *et al.* (1975).

Province 9

The surface sediment layer of Province 9 (Fig. 13) consists of terrigenous mud transported from the nearby rivers and accumulated along the southeast coast of Korea. This layer of silty clays is 40 to 50 m thick lying in water depths of 20 to 50 m. Below 50 m sediment depth, there is a relict sand layer that may extend to 790 m. According to seismic refraction profiles (LUDWIG *et al.,* 1975), these unconsolidated sediments extend to a depth of 1480 m. The sediment column is thicker toward shore and thins toward the axis of the strait. Acoustic basement is rough and consists of sandstone and basalt.

The geoacoustic model for Province 9 presented in Table 6 is derived as described below:

1. The velocity of bottom water is estimated to be 1482 m/s (Fig. 6).

2. A velocity ratio for sediment to bottom water of 0.994 is used to characterize the nearshore muds (MONET and GREENE, 1985).

3. The compressional wave velocity at the surface of the uppermost layer (silty clays) is calculated to be 1473 m/s from items 1 and 2.

4. Compressional wave velocity with depth in the sediments is calculated as follows: for the surface silty clays, $V_p = (1000)(V_{p0} + 1.304Z - 0.741Z^2 + 0.257Z^3)$, where V_{p0} equals 1.535 km/s and Z is depth in *kilometers* (HAMILTON, 1980); for the medium sand layer, $V_p = KZ^{0.015}$, where K is 1736 m/s and Z is depth corrected for consolidation due to overburden pressure; for the sandstone overlying acoustic basement, an interval

velocity of 2940 m/s is used based on LUDWIG *et al.* (1975).

Table 6. Geoacoustic Model for the Strait of Korea, Province 9.

	Depth (m)	V_p (m/s)	V_s (m/s)	K_p (dB/m/kHz)	K_s (dB/m/kHz)	ρ (g/cm^3)
Bottom Water	20-50	1482				
silty	surface	1473	33	0.075	17.3	1.48
clay	5	1480	65	0.078	18.0	1.49
	10	1486	76	0.080	18.5	1.49
	15	1492	88	0.083	19.1	1.50
	20	1499	98	0.085	19.6	1.51
	25	1505	103	0.088	20.3	1.51
	50	1536	144	0.099	22.8	1.55
	75	1847	445	0.377	8.8	2.09
medium	100	1857	488	0.354	8.2	2.09
sand	200	1878	597	0.280	6.5	2.10
	300	1890	661	0.230	5.3	2.10
	400	1898	715	0.194	4.5	2.11
	500	1905	754	0.146	3.4	2.11
	600	1910	793	0.132	3.1	2.12
	700	1915	823	0.118	2.7	2.12
sandstone	800-1500	2940	1350	0.053	1.2	2.20
Acoustic Basement (Sandstone-Basalt)		4350	2142	0.02	0.07	2.43

5. Shear wave velocity with depth in the sediment is calculated using the relationship between effective stress, void ratio and shear modulus developed by BRYAN

and STOLL (1988) and subsequent calculation of velocity by RICHARDSON *et al.* (1991). Laboratory values are converted to field velocities (lab × $\sqrt{2}$) as suggested by STOLL *et al.* (1987). Void ratio is calculated from the density in the table and an assumed value of 2.65 g/cm^3 for grain density.

6. A value for V_s of 1350 m/s is used for the sandstone layer, after HAMILTON (1980).

7. Compressional wave attenuation at the sediment surface is estimated to be 0.075 dB/m/kHz based on porosity values from CHOUGH *et al.* (1991) and the relationship developed by HAMILTON (1980).

8. Compressional wave attenuation with depth in the sediments is calculated as follows: for sediments to 450 mbsf, $K_p(Z) = 0.214 - 0.00014Z - (0.214 - K_{p0})e^{-Z/200}$ with K_{p0} equal to 0.45; for sediments lying between 450 and 1480 mbsf, $K_p(Z) = 0.214 - 0.00014Z$.

9. Shear wave attenuation at the sediment surface is estimated to be 17.3 dB/m/kHz (HAMILTON, 1980).

10. Shear wave attenuation with depth in the sediments is calculated as follows: for the silty clay layer, $K_s(Z) = K_p(Z)(K_{s0}/K_{p0})$; for the medium sand layer, $K_s = 23.3K_p$ based on calculations for Province 8.

11. Densities for the silty clays are calculated from HAMILTON (1978) using the relation $D(Z) = D(0) + 1.395Z - 0.617Z^2$, where $D(0)$ is based on representative data from HAMILTON and BACHMAN (1982) and Z is depth in kilometers. Densities of sand, sandstone, and basalt are based on representative values from HAMILTON (1980).

MODEL APPLICABILITY

The partitioning of the Strait of Korea into geoacoustic provinces as described in this technical note is based on a synthesis of referenced literature and data pertaining *specifically* to this geographic and oceanographic area. The question arises as to whether the results of this study can be extended to other straits.

A variety of factors affecting sedimentation within a strait are regionally specific.

Sedimentary provenance (origin) will vary from strait to strait, affecting the grain size distribution, bulk sediment density, bulk grain density, sedimentation rate and lateral variability of these parameters within the area. Various factors, such as the number, flow rate, and volume outflow of rivers, amount of rain fall, size, vegetative coverage, and sediment type of drainage area, etc., control the rate of sediment supply to a strait. The physical and biological oceanography of the water column influence sedimentation, often to a large degree. Regional tectonic history controls the roughness and composition of the underlying acoustic basement.

Nevertheless, some characteristics of straits are inherently the same. Straits are generally areas of constricted water flow, and, where strong currents exist, great hydrodynamic stress may exist to transport sediments. Impingement of stress on the bottom will redistribute sediment, resulting in a characteristic zonation of surface sediment types into lobes or fields oriented along the axis of transport and thus of the strait itself. Coarser sediment is left as a lag deposit in an area of greater stress, i.e., the main flow channel; finer sediment is deposited distal to the main flow channel in an area where the flow loses competence. Since straits are generally shallower than adjacent basins, hydrodynamic stress usually reaches a large portion of the sea floor in the strait.

Eustatic sea level history imposes a common signature to the sedimentary record of straits by virtue of the shallow nature of straits. Recent (since the Pleistocene) sea level regressions and transgressions resulted in the subaerial exposure of marine sediments in shallow areas. Subsequent inundation and resumption of marine sedimentation often result in acoustic reflectors and layering within the sedimentary column, as observed in the Strait of Korea.

In a general sense, the results of the modeling presented in this technnical note can be applied to straits that meet three basic criteria: presence of rough acoustic basement due to a similar tectonic environment, high levels of sedimentary input on at least one side of the strait, and existence of strong hydrodynamic stress generated by forces near the magnitude of a western boundary current that interacts with the sea floor in the strait. Straits located in a similar tectonic environment are found in areas of increased seismicity such as found along the western Pacific margin, a region of continental-margin-island-arc

and back-arc-basin tectonics. Similar tectonic environment must be coupled with other factors, such high sediment supply and the presence of a strong current. Possible analogs to the Strait of Korea may be the Formosa Strait and straits in the Phillipines and Indonesia.

REFERENCES

BELGODERE, C. and A. LOWRIE (1980). *A geological interpretation of acoustic properties in Korea Strait.* NAVOCEANO Report, July.

BUTENKO, J., J. D. MILLIMAN, and Y.-c.YE (1985). Geomorphology, shallow structure, and geological hazards in the East China Sea. *Continental Shelf Research,* **4,** 121-141.

BRYAN, G. M. and R. D. STOLL (1988). The dynamic shear modulus of marine sediments. *Journal of the Acoustical Society of America,* **83,** 2159-2164.

CHOUGH, S. K. (1983). *Marine geology of Korean seas.* International Human Resources Development Corporation Publishers, Boston, MA, 157pp.

CHOUGH, S. K., K. S. JEONG, and E. HONZA (1985). Zoned facies of mass-flow deposits in the Ulleung (Tsushima) Basin, East Sea (Sea of Japan). *Marine Geology,* **65,** 113-125.

CHOUGH, S. K., H. J. LEE, and S. J. HAN (1991). Sedimentological and geotechnical properties of fine-grained sediments in part of the South Sea, Korea. *Continental Shelf Research,* **11,** 183-195.

HAMILTON, E. L. (1972). Compressional-wave attenuation in marine sediments. *Geophysics,* **37,** 620-646.

HAMILTON, E. L. (1978). Sound velocity-density relations in sea-floor sediments and rocks. *Journal of the Acoustical Society of America,* **63,** 366-377.

HAMILTON, E. L. (1980). Geoacoustic modeling of the sea floor. *Journal of the Acoustical Society of America,* **68,** 1313-1340.

HAMILTON, E. L. and R. T. BACHMAN (1982). Sound velocity and related properties of marine sediments. *Journal of the Acoustical Society of America,* **72,** 1891-1904.

JAPAN OCEANOGRAPHIC DATA CENTER (1968). *CSK Atlas, Vol. 2: Winter 1965-66.* Hydrographic Division, Maritime Safety Agency, Tokyo.

JAPAN OCEANOGRAPHIC DATA CENTER (1971). *CSK Atlas, Vol. 5: April 1967-March 1968.* Hydrographic Department, Maritime Safety Agency, Tokyo.

KATSURA, T. and M. NAGANO (1976). Geomorphology and tectonic movement of the sea floor, northwest off Kyushu, Japan. *Journal of the Oceanographical Society of Japan,* **32,** 139-150.

KELLER, G. H. and Y.-c. YE (1985). Geotechnical properties of surface and near-surface deposits in the East China Sea. *Continental Shelf Research,* **4,** 159-174.

KOREA HYDROGRAPHIC OFFICE (1980). *Bathymetric Chart No 4201, Vicinity of Busan, Korea.* Seoul.

LEE, H. J., S. K. CHOUGH, S. S. CHUN, and S. J. HAN (1991). Sediment failure on the Korea Plateau slope, East Sea (Sea of Japan). *Marine Geology,* **97,** 363-377.

LUDWIG, W. J., S. MURAUCHI, and R. E. HOUTZ (1975). Sediments and structure of the Japan Sea. *Geological Society of America Bulletin,* **86,** 651-664.

MONET, W. F. and R. R. GREENE (1985). *Bottom loss upgrade (BLUG) extensions to strategic shallow water areas: Korea Strait.* Report No. SAIC-85/1825, Science Applications International Corporation, McLean, VA, 96pp.

MURAUCHI, S. and T. ASANUMA (1969). Studies on the seismic profile records of sediments on the continental shelf east of the Tsushima Islands, Kyushu, Japan. *Memoirs of the National Science Museum,* **2,** Ueno Park, Tokyo.

NAVAL OCEANOGRAPHIC OFFICE (1974). *Oceanographic survey report, Sea of Japan,* U.S. Naval Oceanographic Office Special Publication **133-18-1**, 167 pp.

PARK, S. C. and D. G. YOO (1988). Depositional history of Quaternary sediments on the continental shelf off the southeastern coast of Korea (Korea Strait). *Marine Geology,* **79,** 65-75.

PARK, S. H. (1983). *Underwater acoustic propagation in the Korea Strait.* Master's Thesis, Naval Postgraduate School, Monterey, CA, 135pp.

PARK, Y. A. and B. K. KHIM (1990). Clay minerals of the recent fine-grained sediments on the Korean continental shelves. *Continental Shelf Research,* **12,** 1179-1191.

RICHARDSON, M. D., E. MUZI, L. TROIANO, and B. MIASCHI (1991). Sediment shear waves: A comparison of in situ and laboratory measurements. In, R. H. BENNETT, W. R. BRYANT, and M. H. HULBERT (eds.), *Microstructure of fine-grained sediments,* Springer-Verlag, New York, pp. 403-415.

SHEPARD, F. P., K. O. EMERY, and H. R. GOULD (1949). Distribution of sediments on East Asiatic continental shelf. *Allan Hancock Foundation Publications Occasional Paper,* **9**, University of Southern California Press, Los Angeles, CA, 64pp.

STOLL, R. D., G. M. BRYAN, R. FLOOD, D. CHAYES, and P. MANLEY (1987). Shallow seismic experiments using shear waves. *Journal of the Acoustical Society of America,* **83,** 93-102.

TIMES BOOKS (1980). *The Times Atlas of the World, Comprehensive Edition,* 6th ed., New York.

FIGURES

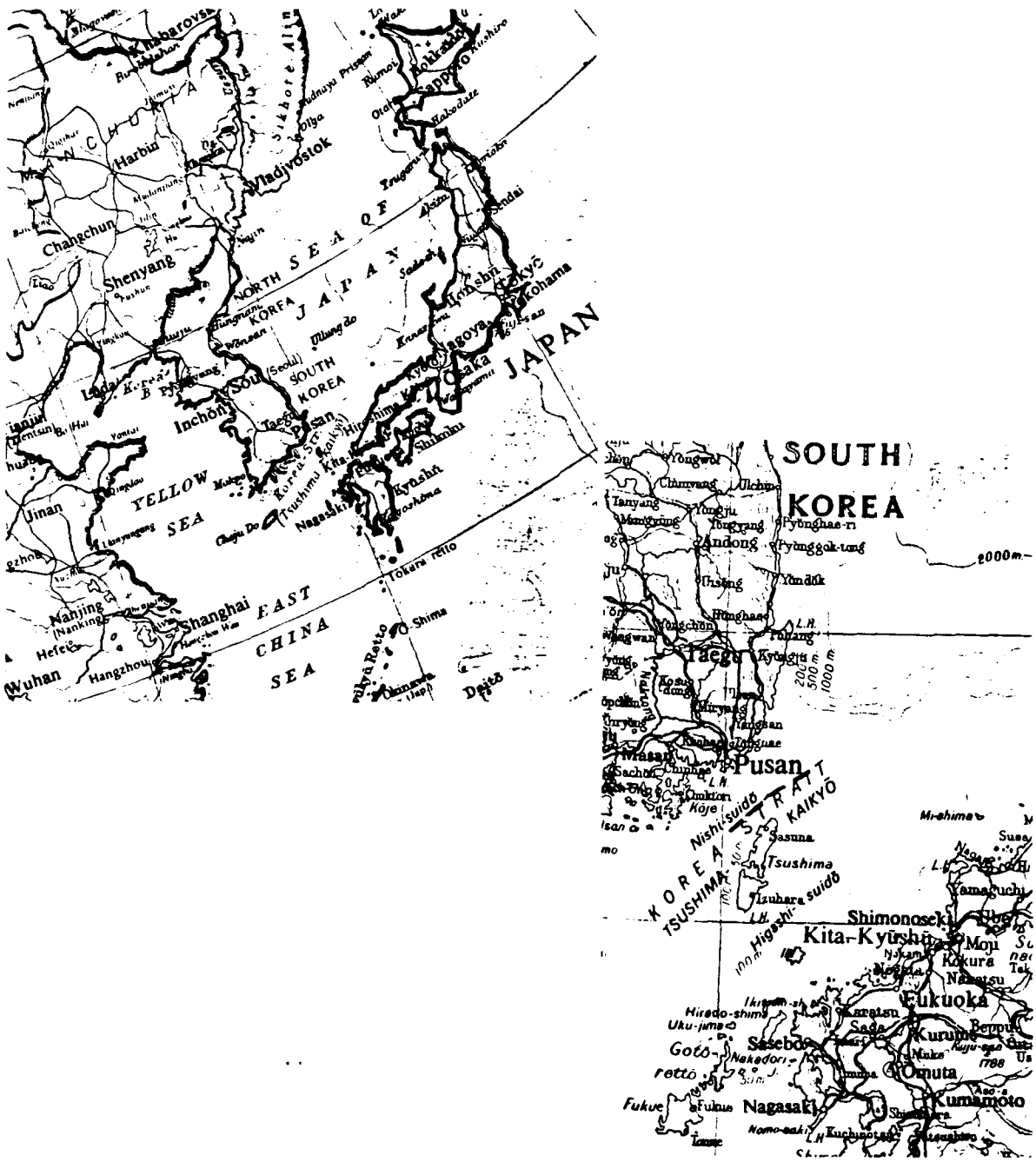

Figure 1. Map of South Korea, Strait of Korea (Tsushima Strait), and southwestern Japan. (Figure taken from The Times Atlas of the World, Comprehensive Edition, 1980.)

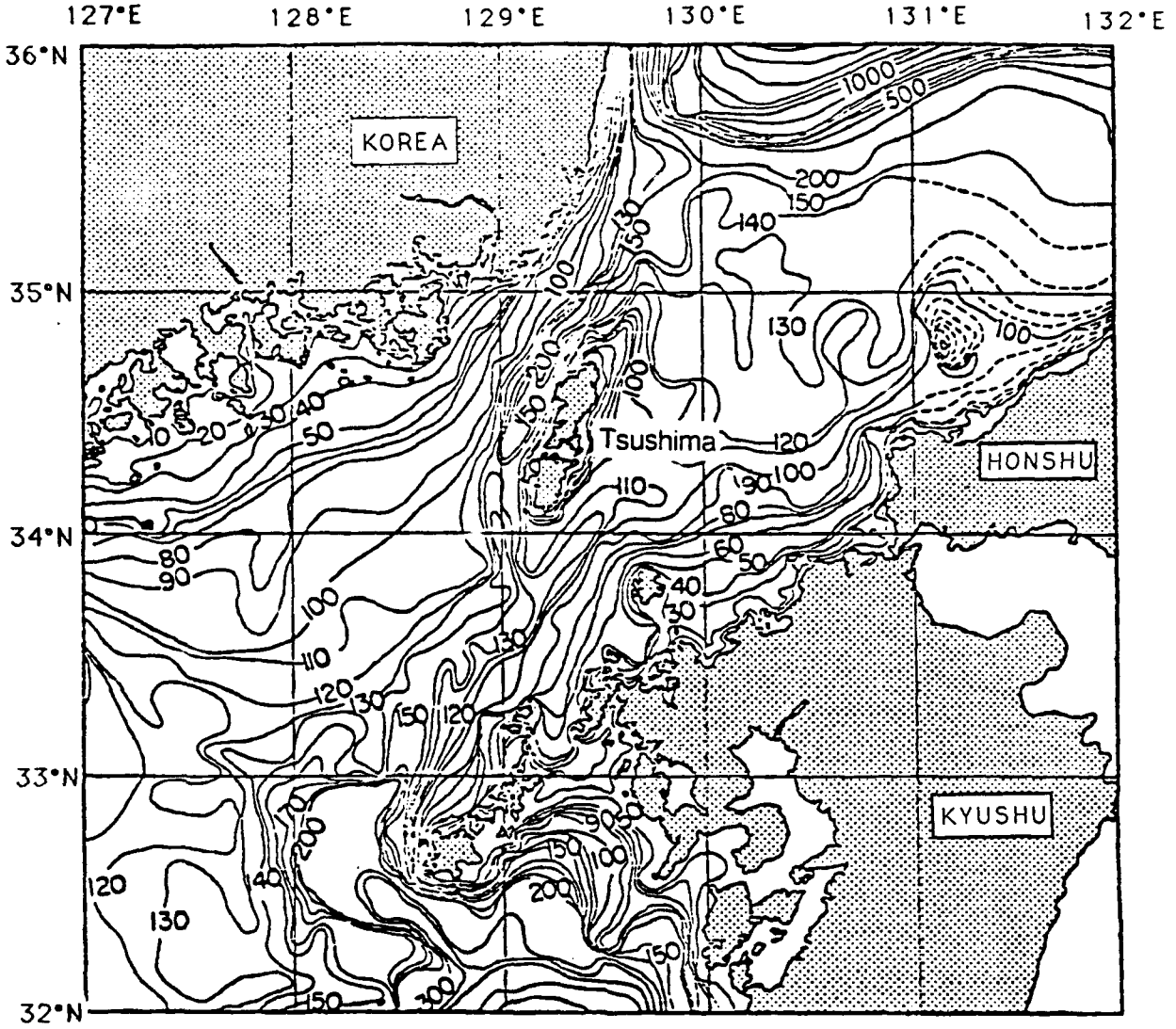

Figure 2. Bathymetry, in meters, for the Strait of Korea. (Figure taken from Monet and Greene, 1985; originally published in Belgodere and Lowrie, 1980.)

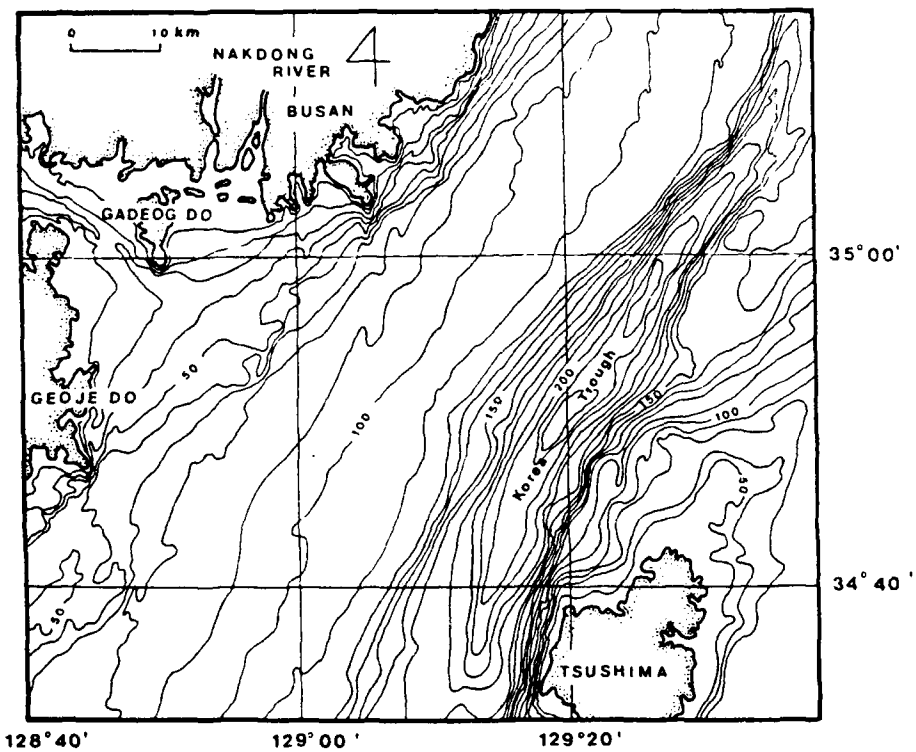

Figure 3. Bathymetry in the region between Korea and Tsushima Island. (Figure from Park and Yoo, 1988, who adapted it from Korea Hydrographic Office, 1980).

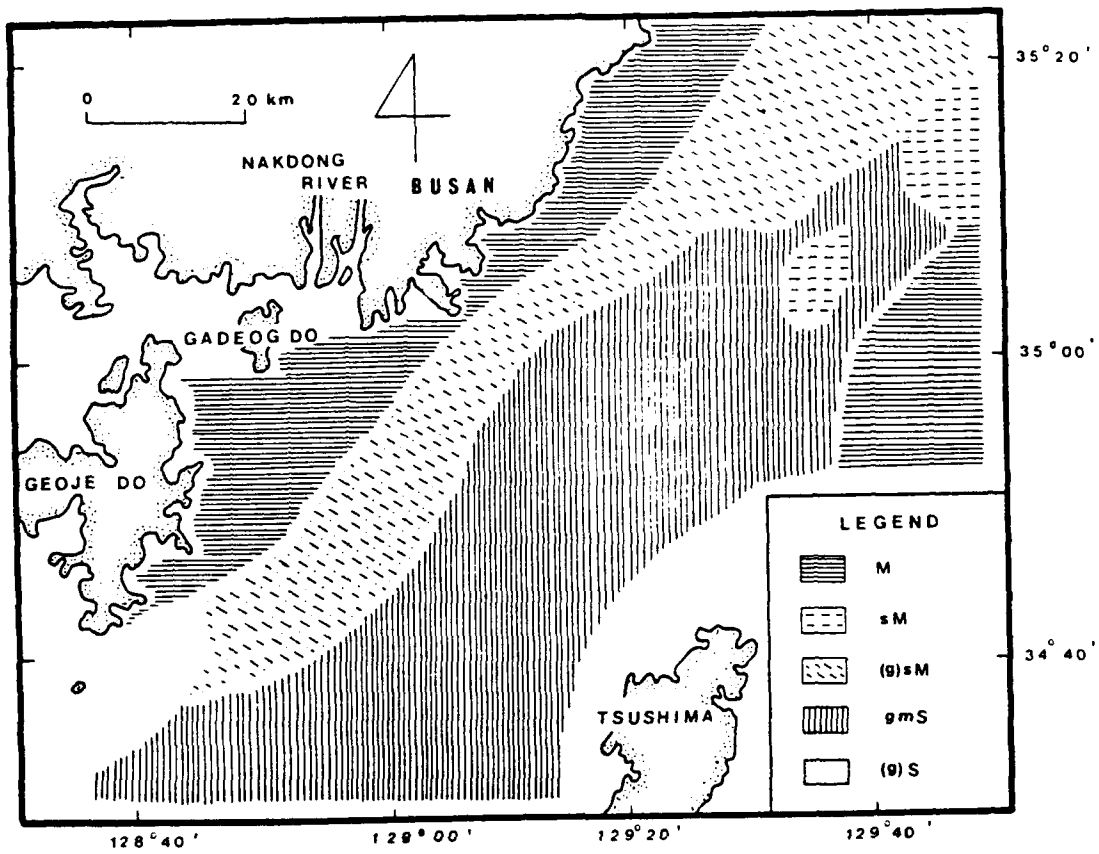

Figure 4. Distribution of surface sediment types in the region between Korea and Tsushima Island. Legend symbols designate: M, mud; sM, sandy mud; (g)sM, gravelly sandy mud; gmS, gravelly muddy sand; (g)S, gravelly sand. (Figure taken from Park and Yoo, 1988.)

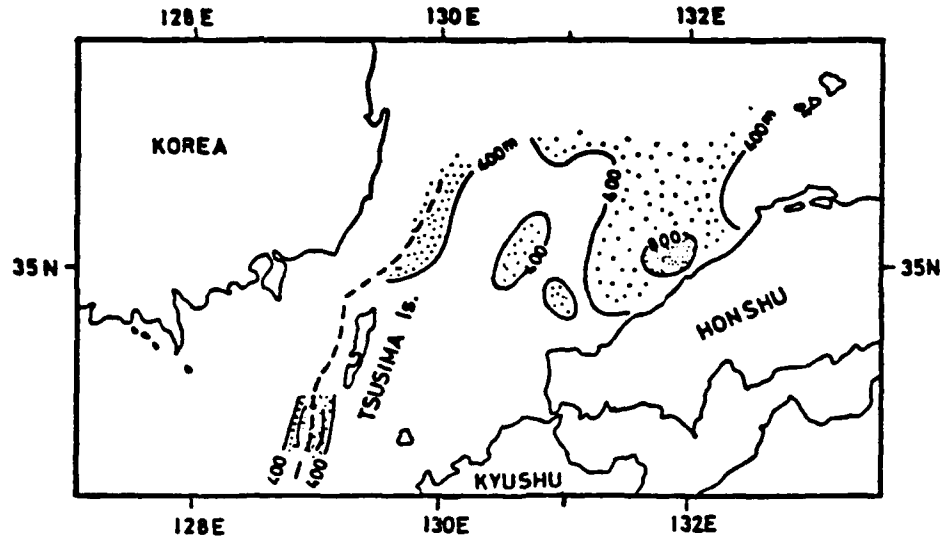

Figure 5. Isopach map of unconsolidated sediments. Dotted areas depict regions covered by unconsolidated sediments thicker than 400 m. Korea Trough (or Tsushima Trough) is shown by the dashed line. (Figure from Monet and Greene, 1985; originally from Murauchi et al., 1969.)

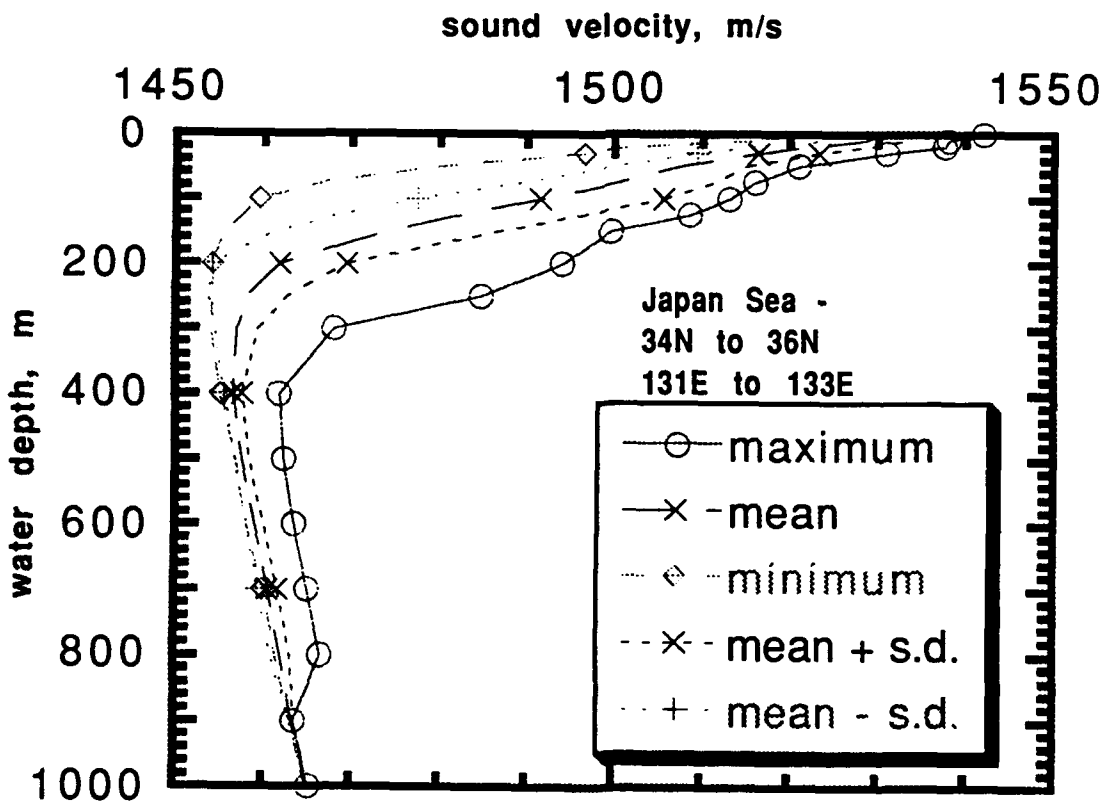

Figure 6. Sound velocity in meters/second versus depth in the water column for region in the Japan Sea just north of the Strait of Korea. (Data courtesy of J. Soileau, NOARL.)

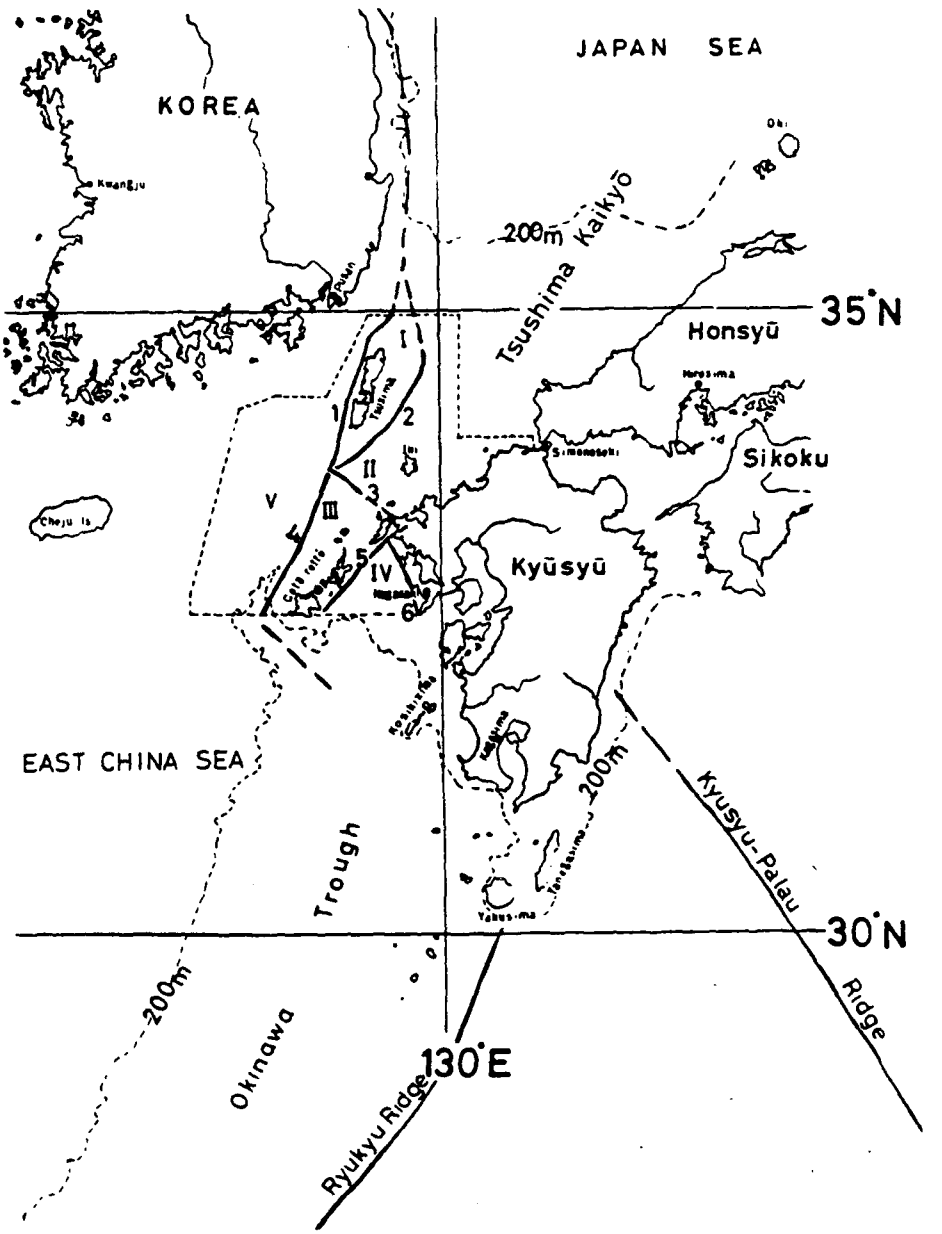

Figure 7. Major tectonic lines and tectonic provinces in the Strait of Korea. 1. Tsushima Tectonic Line; 2. Iki Tectonic Line; 3. Hiratonic Line; 4. Goto Tectonic Line; 5. Ainoshima Fault; 6. Yobuko-no-seto Fault; I. Tsushima Province; II. Iki Province; III. Goto Province, IV. Ainoshima Province; V. Tounghai Shelf Province. (Figure from Katusura and Nagano, 1976.)

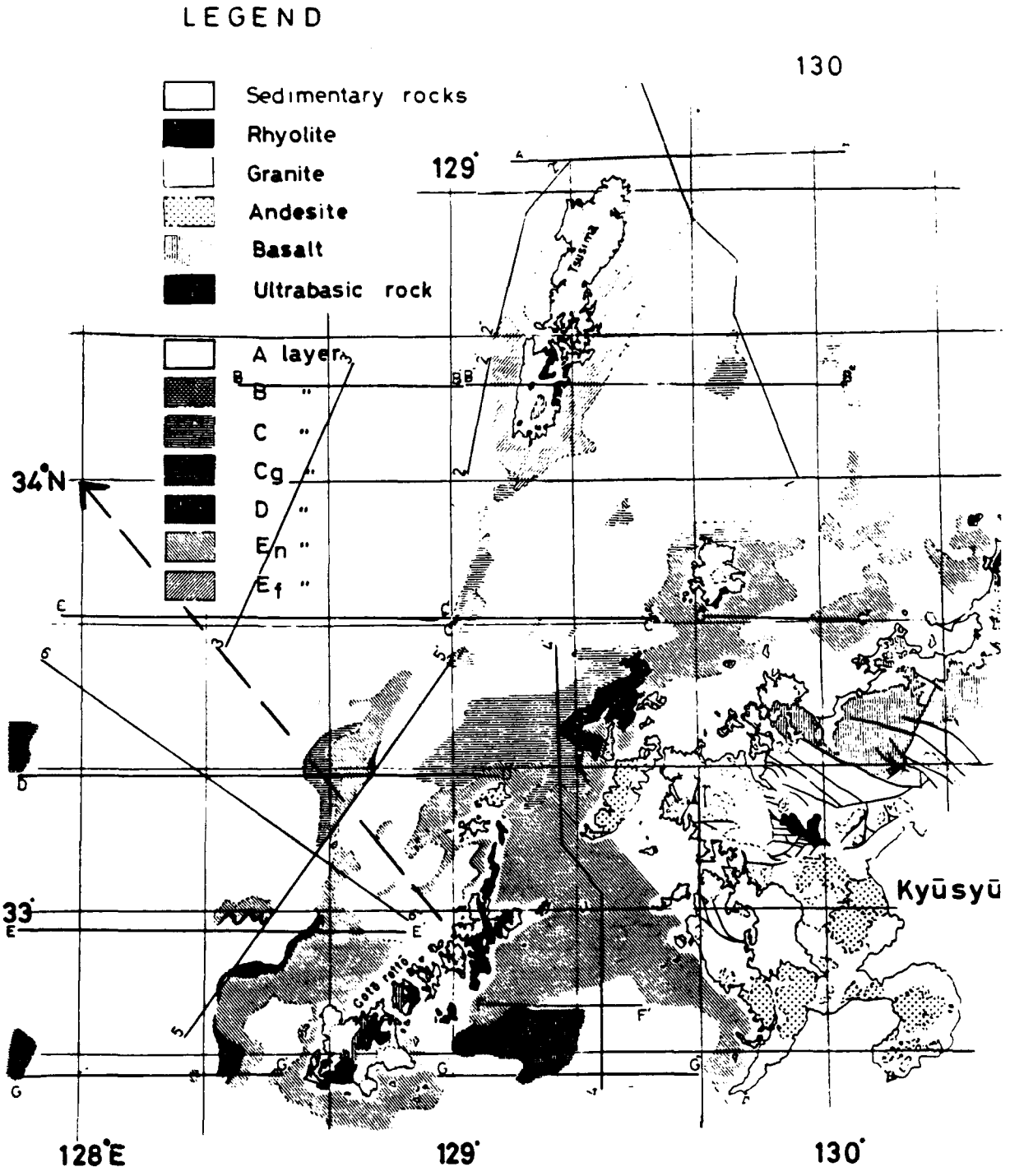

Figure 8a. Submarine and land geology of the Japan side of the Strait of Korea. Dashed arrow shows the eastern part of the transect modeled in this technical note. Solid lines represent the track lines of seismic sections. See Table 1 for descriptions of sedimentary sequences A through Ef. (Figure, which is reproduced as well as the original journal figure permits, is taken from Katsura and Nagano, 1976.)

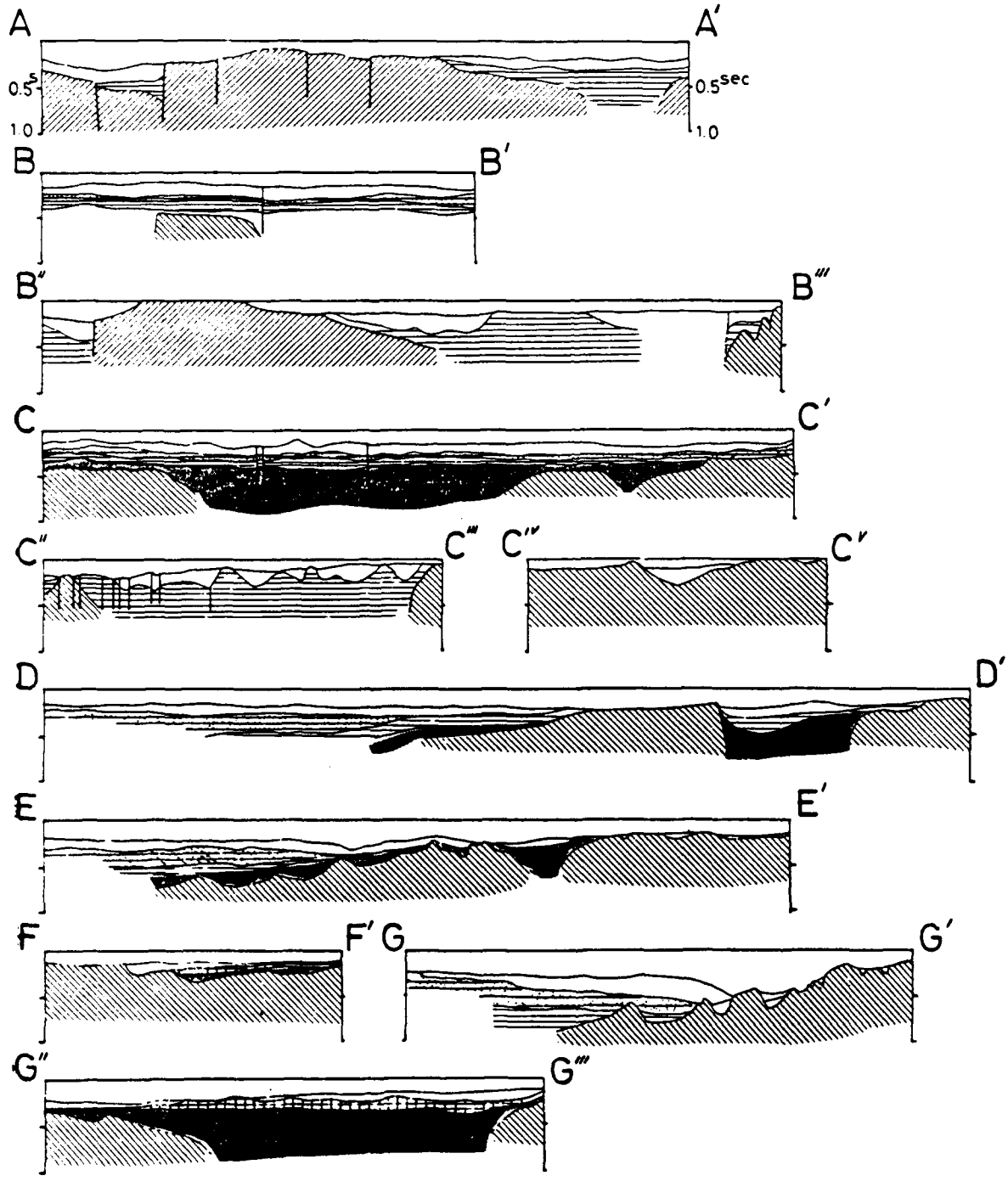

Figure 8b. Seismic section interpretations for east-west tracks. (Figure from Katsura and Nagano, 1976.)

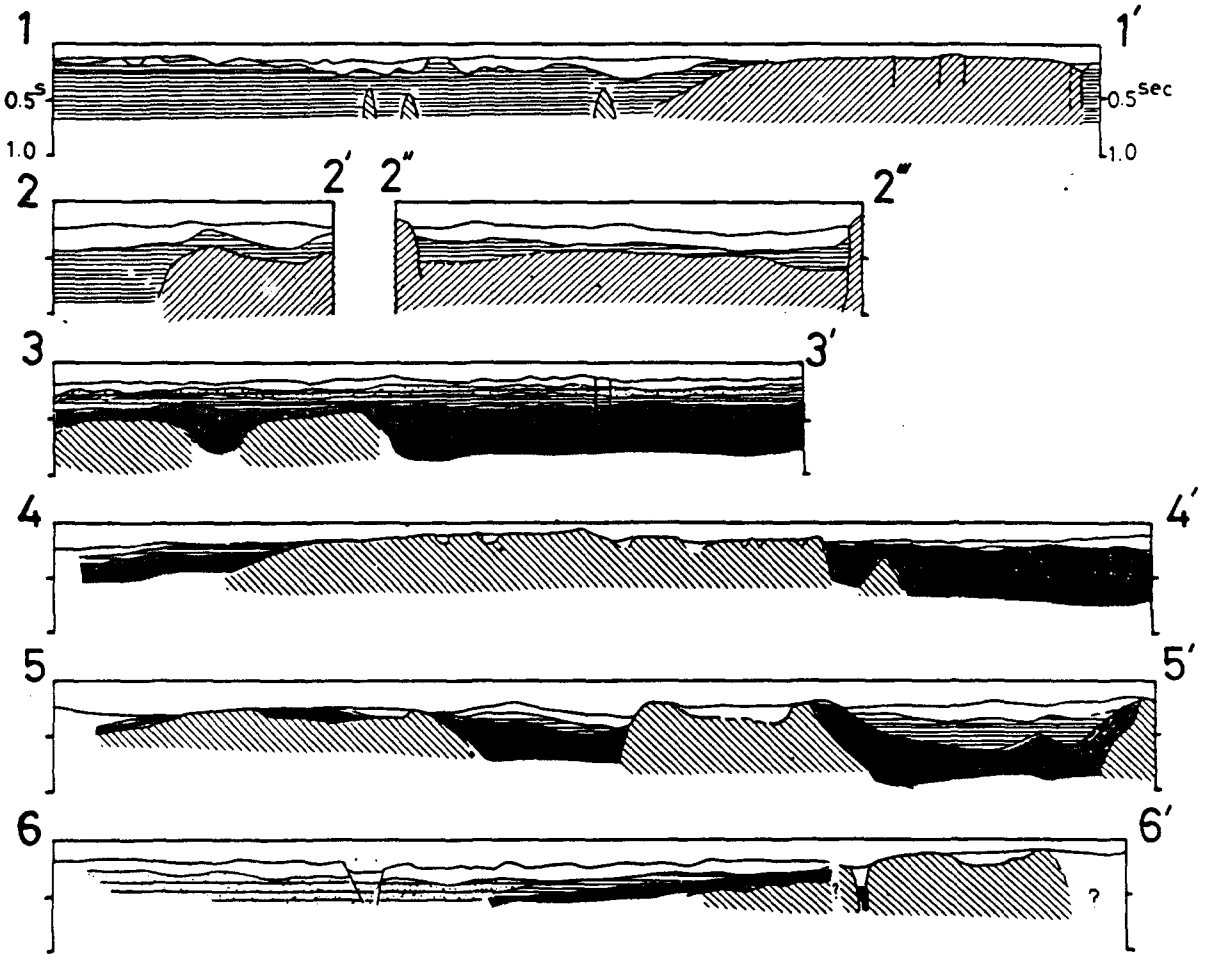

Figure 8c. Seismic section interpretations for oblique tracks. (Figure from Katsura and Nagano, 1976.)

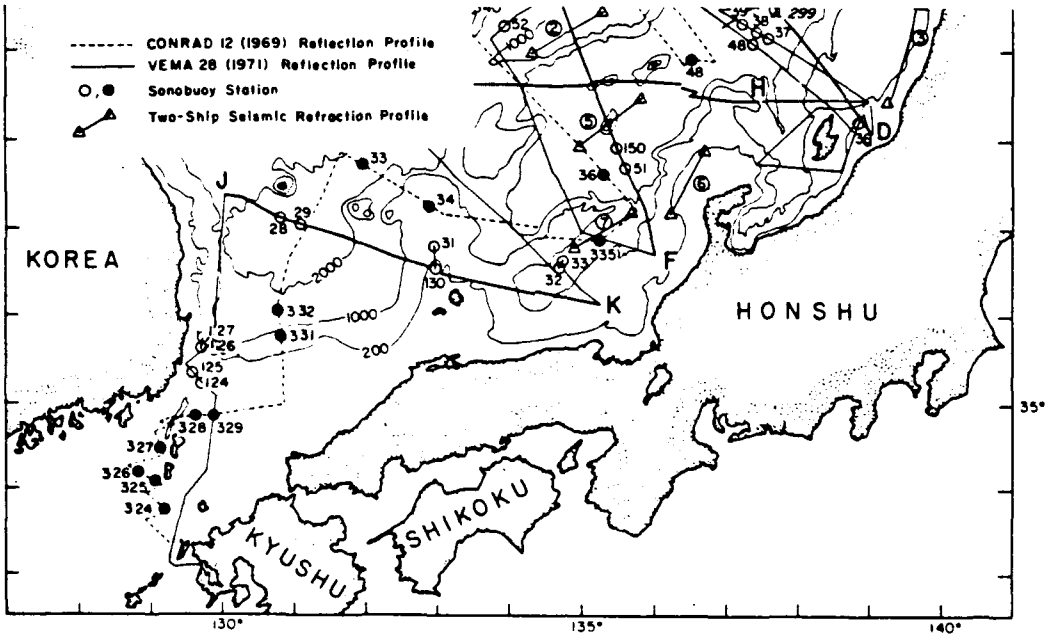

Figure 9a. Location of sonobuoy stations in the Japan Sea and Strait of Korea. Contours are in meters. (Figure from Ludwig et al., 1975.)

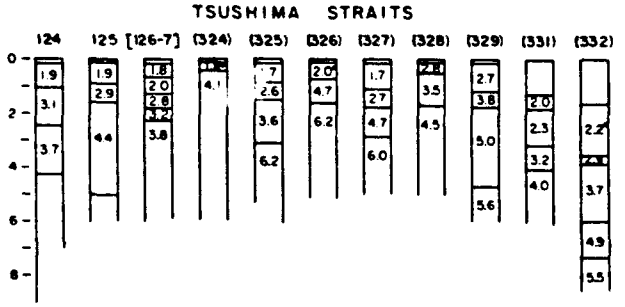

Figure 9b. Velocity structure sections from sonobuoy stations. Velocities are in km/sec. Bracketed station numbers indicate the velocities for that station are true velocities since a reversed pair of refraction profiles was used. A parenthesized station number indicates an unreversed refraction profile computed by assuming horizontal layers. An asterisk indicates an assumed velocity for masked layers. All other velocities are from wide-angle reflection data and are internal velocities. (Figure from Ludwig et al., 1975.)

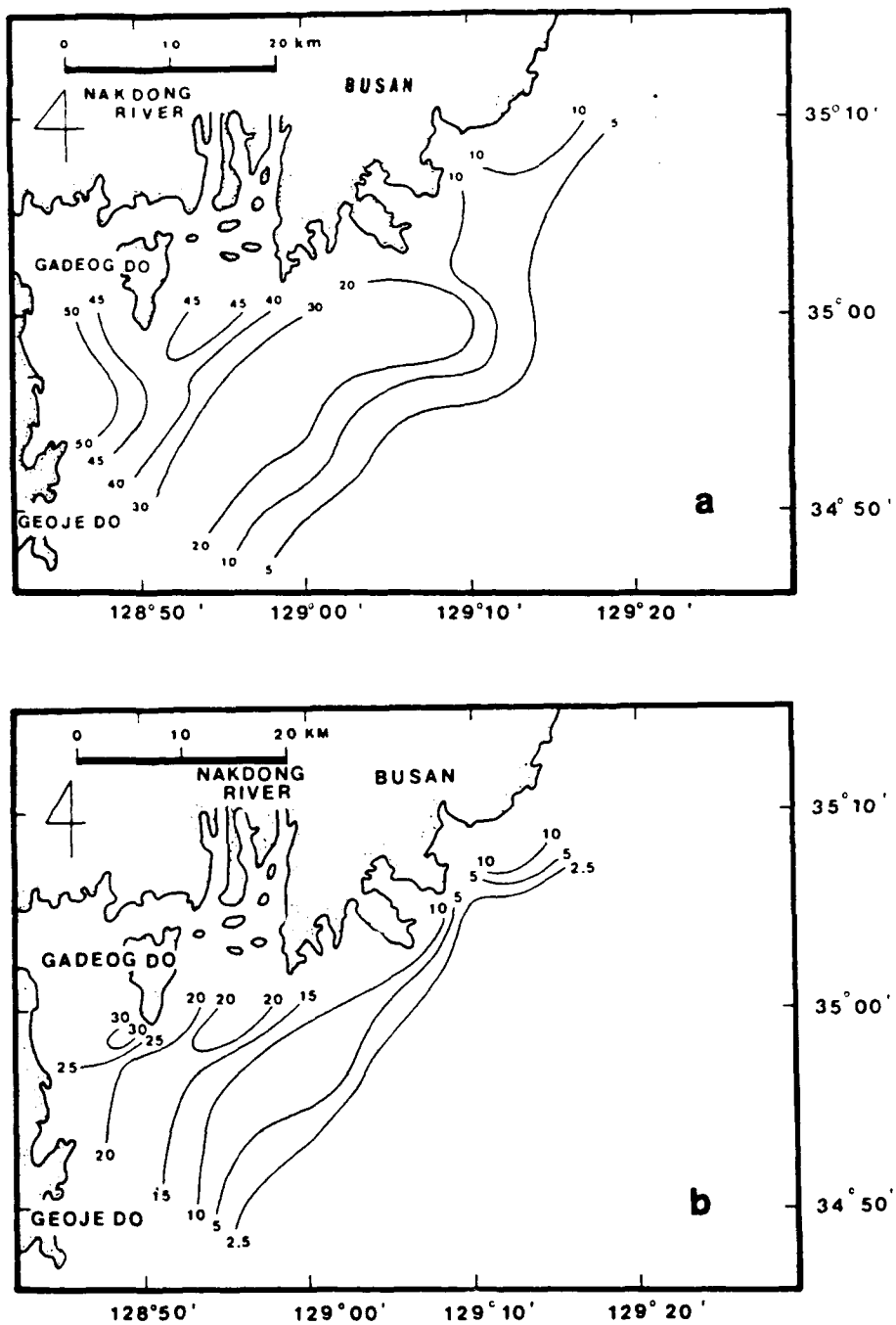

Figure 10. a. Isopach map showing the present-day total sediment thickness in meters above acoustic basement.

b. Isopach map showing the Holocene sediment thickness (sequence A in Fig.11, b and c) in meters above acoustic basement. (Both figures from Park and Yoo, 1988.)

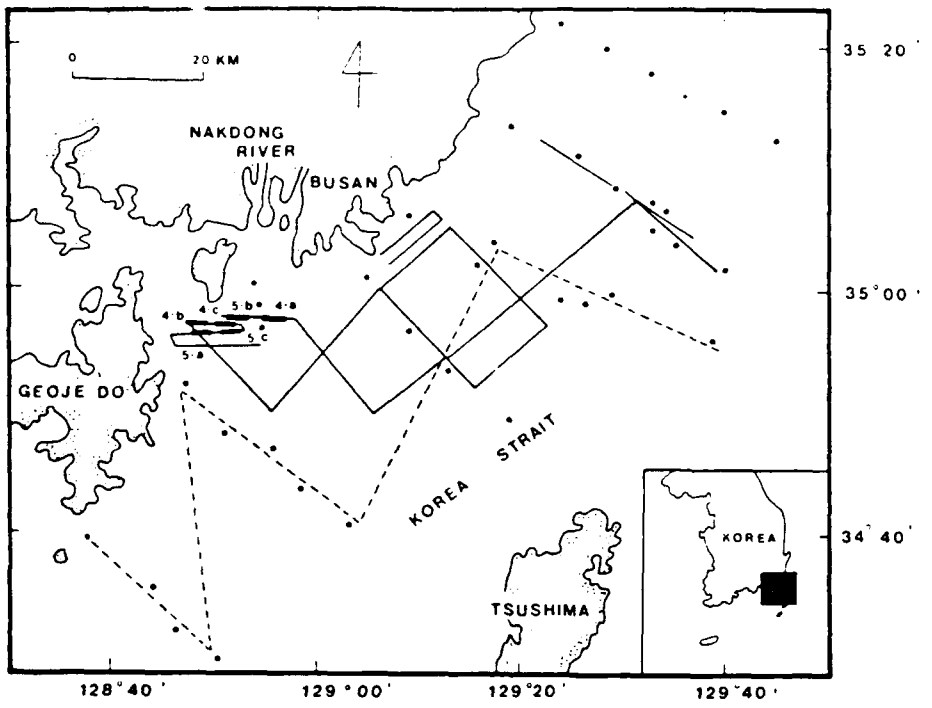

Figure 11a. Solid lines indicate the position of Uniboom profiles; dashed lines show the position of side scan sonar and 3.5 kHz subbottom profiles. Circles show location of sampling stations. (Figure taken from Park and Yoo, 1988.)

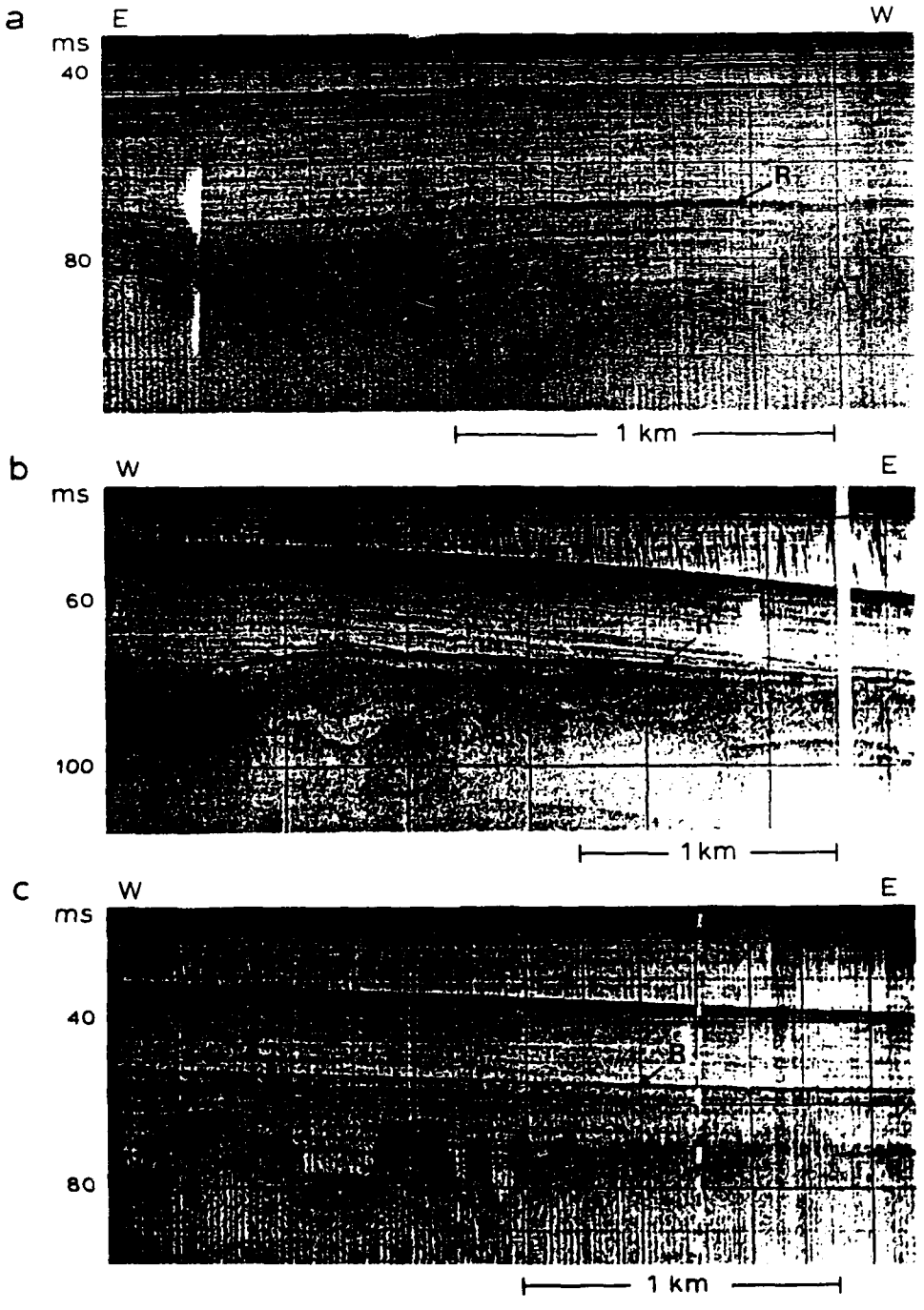

Figure 11b. High resolution seismic profiles for the 4a through 4c track lines showing two major sedimentary sequences separated by a midreflector (R). Designations correspond to the following: A and B, two sedimentary sequences; CH, channel fill structure; F, foreset bedding; AB, acoustic basement. The two-way travel time is shown in milliseconds; 10 ms corresponds to approximately 8 m of sediment. (Figure taken from Park and Yoo, 1988.)

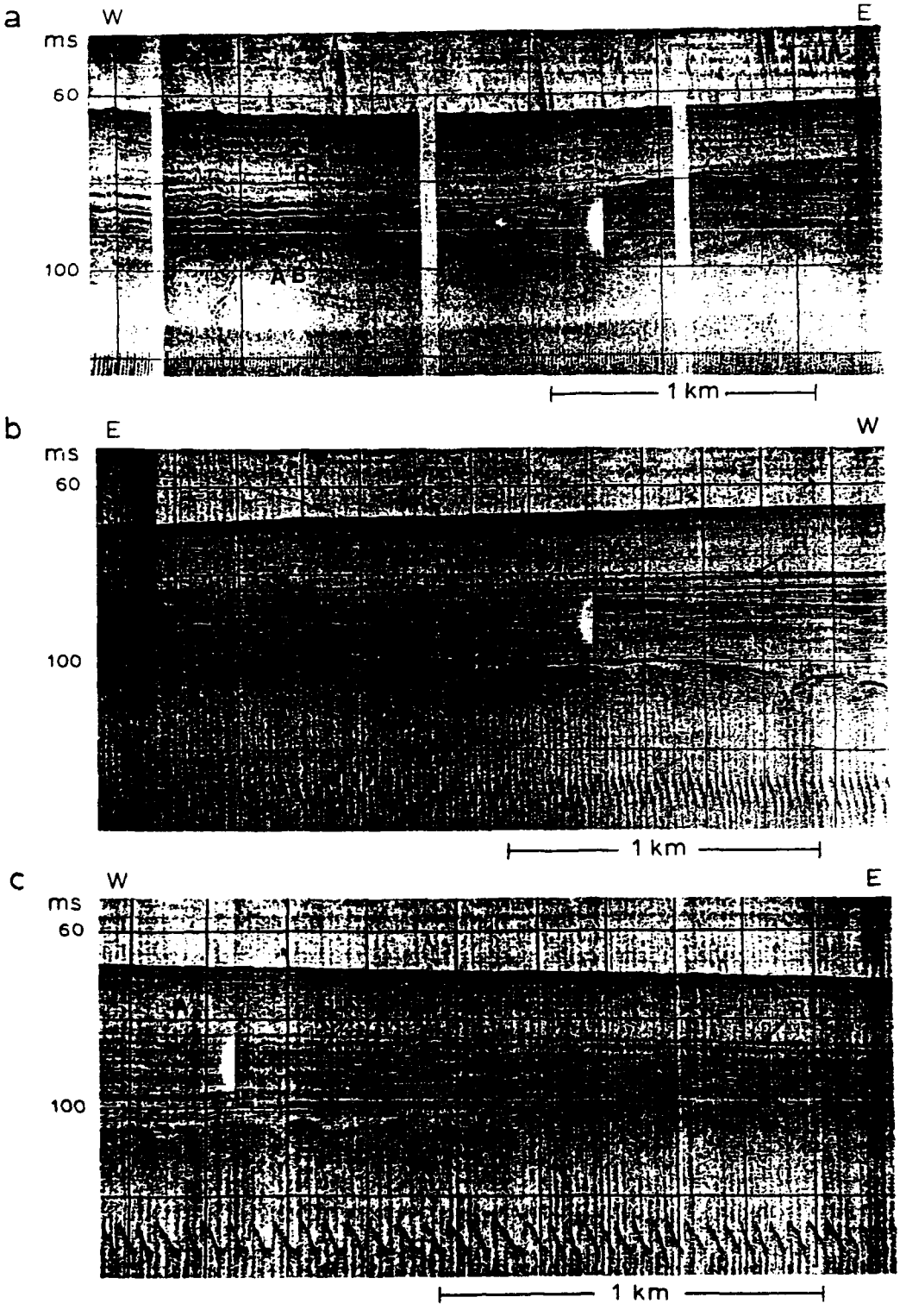

Figure 11c. High resolution seismic profiles for the 5a through 5c track lines showing two sedimentary sequences separated by a midreflector. AT indicates an acoustically turbid layer. (Figure taken from Park and Yoo, 1988.)

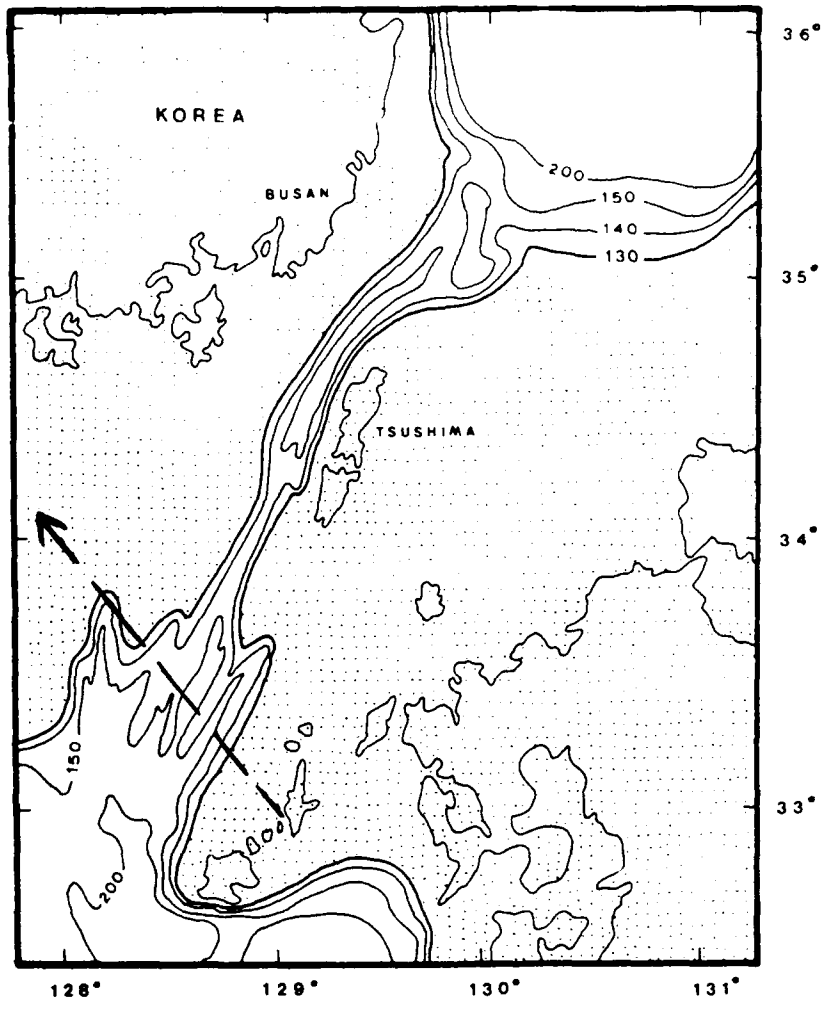

Figure 12. The stippled area shows the subaerially exposed land surface during the last glacial period when sea level was approximately 130 m lower than the present level. Dashed arrow shows the transect on which the geoacoustic model of this technical note is based. (Figure taken from Park and Yoo, 1988, who adapted it from Katsura and Nagano, 1982.)

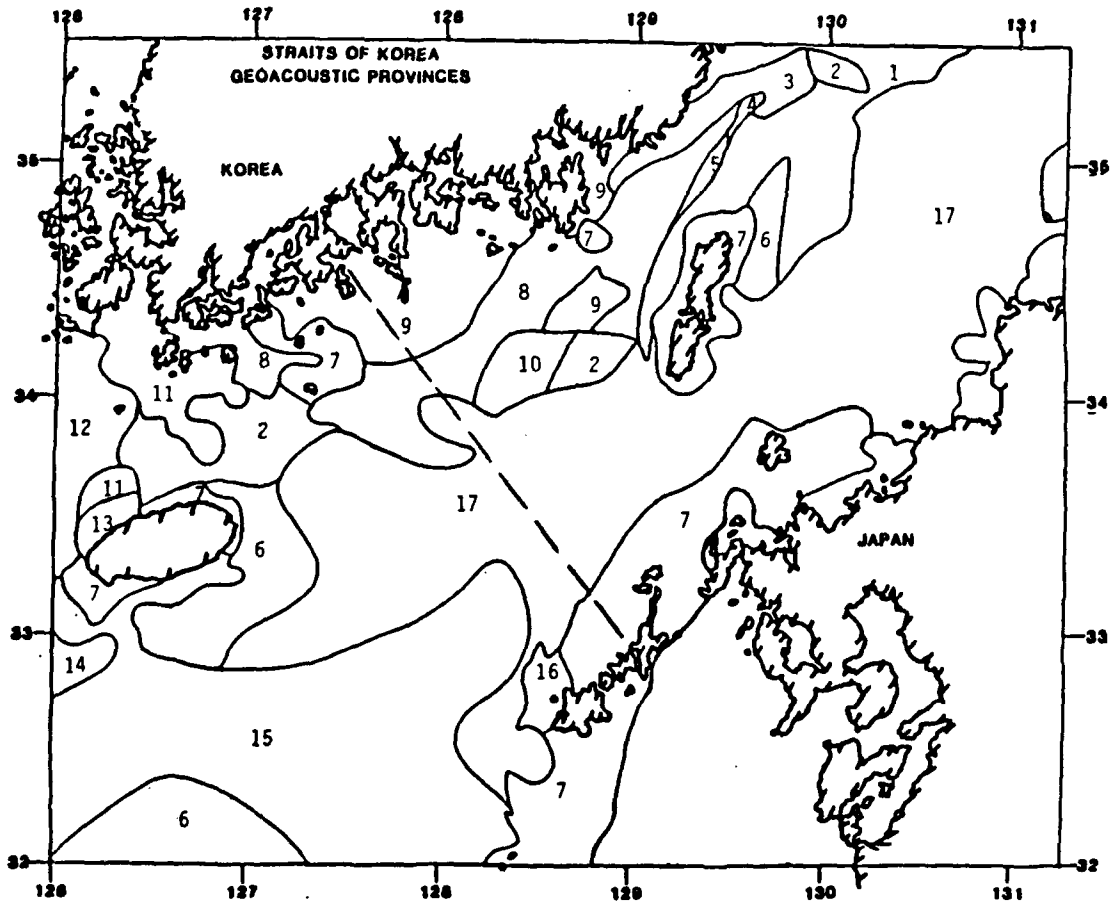

Figure 13. Map of the 17 geoacoustic provinces of the Strait of Korea as defined in this technical note. Four provinces are traversed by the transect (dashed line) modeled in detail. (Figure adapted from Monet and Greene, 1985.)

APPENDIX A

MODEL OF MONET AND GREENE (1985)

Table A1. Characteristics exhibited by 52 geoacoustic provinces shown in Figure A1. (Table from Monet and Greene, 1985.)

	GRAIN SIZE													SED THICK			BASE ROUGH		LAYERING			BATHY	
	SILTY-CLAY	CLAYEY-SILT	SAND-SILT-CLAY	SANDY SILT	SILTY SAND	FINE SAND	COARSE SAND	GRAVELLY SAND	SAND	GRAVELLY ROCK	ROCK	LITTLE OR NONE	THIN	THICK	SMOOTH	ROUGH	PRESENT	NOT PRESENT	SMOOTH	ROUGH
1				●										●	●		●			●
2							●							●		●		●		●
3	●													●		●		●		●
4					●									●		●		●		●
5						●								●		●		●		●
6				●										●	●		●		●	
7			●											●	●		●		●	
8									●			●				●		●	●	
9				●									●			●		●	●	
10									●			●				●		●	●	
11			●										●			●		●	●	
12	●												●			●		●	●	
13							●							●		●		●		●
14					●								●			●		●	●	
15	●												●			●		●	●	
16									●							●		●	●	
17									●			●				●		●		●
18			●										●			●		●		●
19								●					●			●		●		●
20							●						●			●		●		●
21			●										●			●		●		●
22									●			●				●		●		●
23			●											●		●		●		●
24							●							●		●		●	●	
25								●					●			●		●		●
26		●											●			●		●		●
27									●			●				●		●		●
28									●			●				●		●		●
29	●													●		●	●		●	
30			●											●		●	●		●	
31			●											●		●	●			●
32						●							●			●	●			●
33										●		●				●		●	●	
34									●			●				●		●	●	
35						●								●		●		●		●
36						●								●		●		●		●
37			●										●			●		●		●
38						●							●			●		●	●	
39								●					●			●		●		●
40	●												●			●		●		●
41								●					●			●		●		●
42			●										●			●		●		●
43			●									●				●		●		●
44											●	●				●		●		●
45										●		●				●		●		●
46										●		●				●		●		●
47										●		●				●		●		●
48			●										●			●	●			●
49										●		●				●		●		●
50			●											●		●	●		●	
51									●			●				●		●	●	
52							●							●		●	●		●	

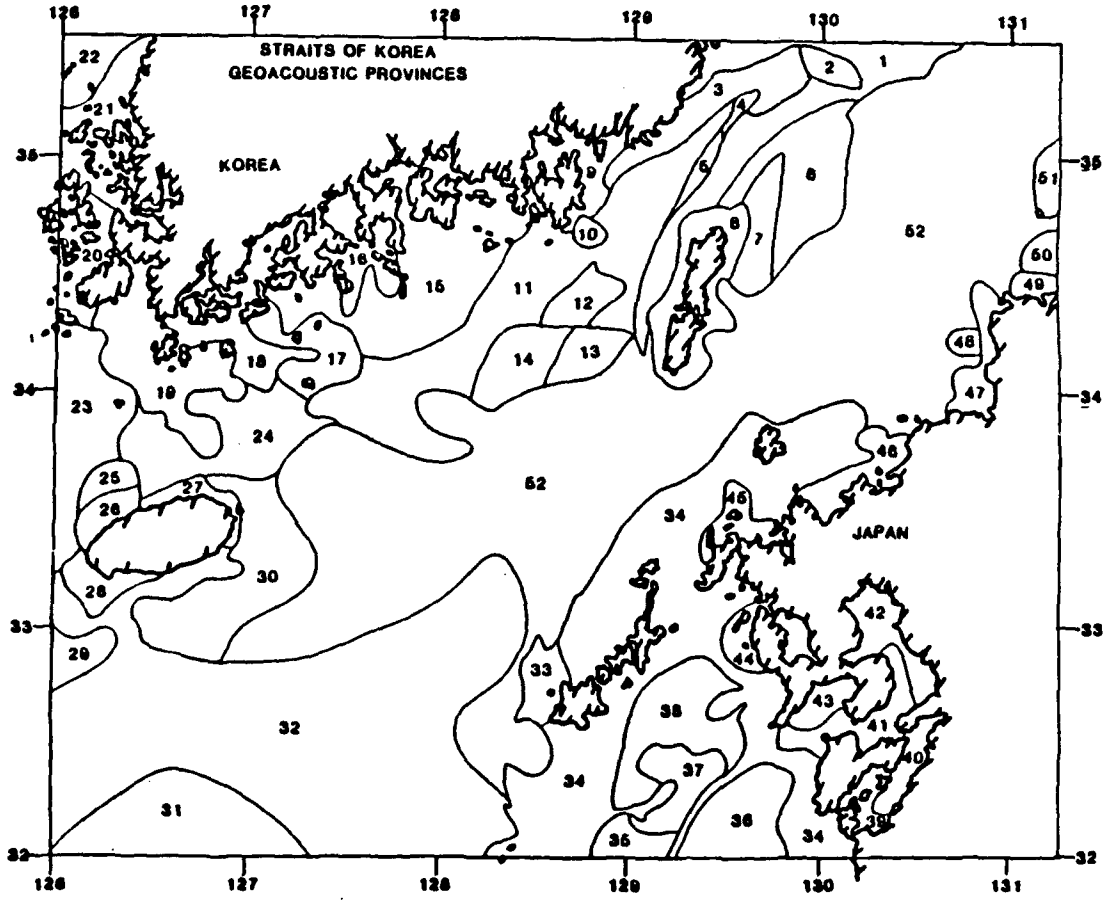

Figure A1. Map of 52 geoacoustic provinces defined by Monet and Greene, 1985. (Figure taken from Monet and Greene, 1985.)

Table A2. Bottom/water velocity ratios. The number designating the sediment province and the corresponding sediment compressional wave velocity ratio as assigned by MONET and GREENE (1985), except where noted by an asterisk (*). Those values noted by asterisks are calculated from alternate sources of geological data. The value is the ratio of the sediment sound velocity to the water sound velocity immediately over the sediment.

Province	V_p Ratio
1	1.033
2	1.201
3	0.994
4	1.078
5	1.145
6	1.145
7	1.201*
8	1.036*
9	0.994
10	1.078
11	1.300
12	1.033
13	1.014
14	0.994
15	1.145
16	3.430
17	1.200*

APPENDIX REFERENCES

MONET, W. F. and R. R. GREENE (1985). *Bottom loss upgrade (BLUG) extensions to strategic shallow water areas: Korea Strait.* Report No. SAIC-85/1825, Science Applications International Corporation, McLean, VA, 96pp.

DISTRIBUTION LIST

Naval Oceanographic and Atmospheric Research Laboratory
Stennis Space Center, MS 39529-5004
Attn: Code 200
240
244 R. Field
W. Kinney
300
360
361 K. Briggs (10)
K. Fischer (10)
113
125L (10)
125P

NAVOCEANO
Stennis Space Center, MS 39522-5001
Attn: Library (2)
Code TD

Naval Research Laboratory
Washington, DC 20375
Attn: Library

REPORT DOCUMENTATION PAGE

Form Approved
OBM No. 0704-0188

1. Agency Use Only *(Leave blank).*	2. Report Date.	3. Report Type and Dates Covered.
	October 1991	Final

4. Title and Subtitle.
Geoacoustic Model of the Strait of Korea

5. Funding Numbers.

Program Element No.	0601153N
Project No.	3202
Task No.	340
Accession No.	DN257015
Work Unit No.	13621V

6. Author(s).
K. B. Briggs and K. M. Fischer

7. Performing Organization Name(s) and Address(es).
Naval Oceanographic and Atmospheric Research Laboratory
Ocean Science Directorate
Stennis Space Center, Mississippi 39529-5004

8. Performing Organization Report Number.
NOARL Technical Note 218

9. Sponsoring/Monitoring Agency Name(s) and Address(es).
Naval Oceanographic and Atmospheric Research Laboratory
Ocean Acoustics and Technology Directorate
Stennis Space Center, Mississippi 39529-5004

10. Sponsoring/Monitoring Agency Report Number.
NOARL Technical Note 218

11. Supplementary Notes.

12a. Distribution/Availability Statement.
Approved for public release; distribution is unlimited.

12b. Distribution Code.

13. Abstract *(Maximum 200 words).*

Understanding the geology of the Strait of Korea is critical in making predictions of acoustic response because the region is a shallow-water, bottom-interacting area. The sediments are predominantly terrigenous with a significant marine biogenic component and exhibit a wide range of textures. In general, sediments are distributed along the axis of the strait by means of strong currents that winnow fines and leave predominantly coarser material as the lag deposit. However, a conspicuous mud belt of silty clay derived from nearby rivers persists near the Korean shore. This deposit thins toward the center of the strait where relict fine and medium sands are exposed. On the Japan side of the strait, hydrodynamic stress from currents waft away finer sediment to expose rock and leave coarse material such as shells in surface sediments. Over most of the strait, recent sea level changes have produced a middepth reflector beneath unconsolidated surface sediments. This acoustic horizon demarcates the surface of previously subaerially exposured marine sediments. Below the approximately 1 km thick layer of sediments in the strait, acoustic basement is rough due, in a large part, to the extensional tectonism associated with the back-arc-basin environment of the nearby Sea of Japan. Acoustic basement consists of folded sandstone or faulted basalt with extrusively and intrusively emplaced volcanic rock.

In this study, the seafloor of the strait is differentiated into 17 provinces based on sediment type, sediment thickness, and presence or absence of layering. A transect from the Goto Islands in Japan to the Kohung Peninsula in Korea was selected to model in detail. This transect traverses four of the largest geoacoustic provinces and samples the range of environments found within the strait. Acoustic property data as a function of depth in the sediment are supplied for each province for use as input parameters to acoustic field models that incorporate the variation of sediment physical properties with depth.

14. Subject Terms.
Bahamas, Straits of Korea, Geoacoustic Parameters, Velocity

15. Number of Pages.
45

16. Price Code.

17. Security Classification of Report.	18. Security Classification of This Page.	19. Security Classification of Abstract.	20. Limitation of Abstract.
Unclassified	Unclassified	Unclassified	SAR